CHAPTER 7

RESULTS AND DISCUSSION

Our experimental results on aluminium diffusion in the elemental semiconductors silicon and germanium, as well as in the compound semiconductors gallium arsenide, indium phosphide and indium antimonide are discussed in this chapter.

For the in-diffusion investigation thin aluminium films were deposited onto the cleaned semiconductor surfaces and isochronally annealed at elevated temperatures. Thin films are commonly used as diffusion sources. However, this method has the disadvantage that a thin native oxide layer can build up instantaneously after cleaning the semiconductor before depositing the aluminium film. Such an oxide layer at the interface between the semiconductor and the thin film creates a diffusion barrier, which reduces the in-diffusion.

Additional measurements were made for comparison of the results, where the diffusion source was introduced into the semiconductors by ion implantation. Here the diffusion source is directly in contact with the investigated material. However, implantations at room temperature create point and extended defects that can also influence the diffusion behaviour dramatically. By implanting the diffusant at elevated temperatures such radiation-induced defects can largely be avoided.

All three methods described were applied on every semiconductor in this study.

7.1. SILICON

Many research results on aluminium diffusion in silicon were reported in recent years. However, the obtained diffusion coefficients were spread over a wide range. This study was performed to investigate the diffusion behaviour up to 900 °C. After annealing a sample with an aluminium film at 1000 °C complete surface oxidation was observed despite a vacuum better than 10^{-7} mbar during annealing. In order to compare results from all three methods annealing temperatures were kept below $T_a \leq 900$ °C.

Our results are compared with coefficients obtained after extrapolating previously reported results to this temperature (see chapter 6.1.).

7.1.1. ALUMINIUM DIFFUSION INTO SILICON

The aluminium diffusion into Si <100> at temperatures up to 900 °C was investigated. An aluminium film of 20 ± 3 *nm* thickness was deposited onto a cleaned Si <100> wafer surface. Samples from this wafer were analysed before and after different annealing cycles.

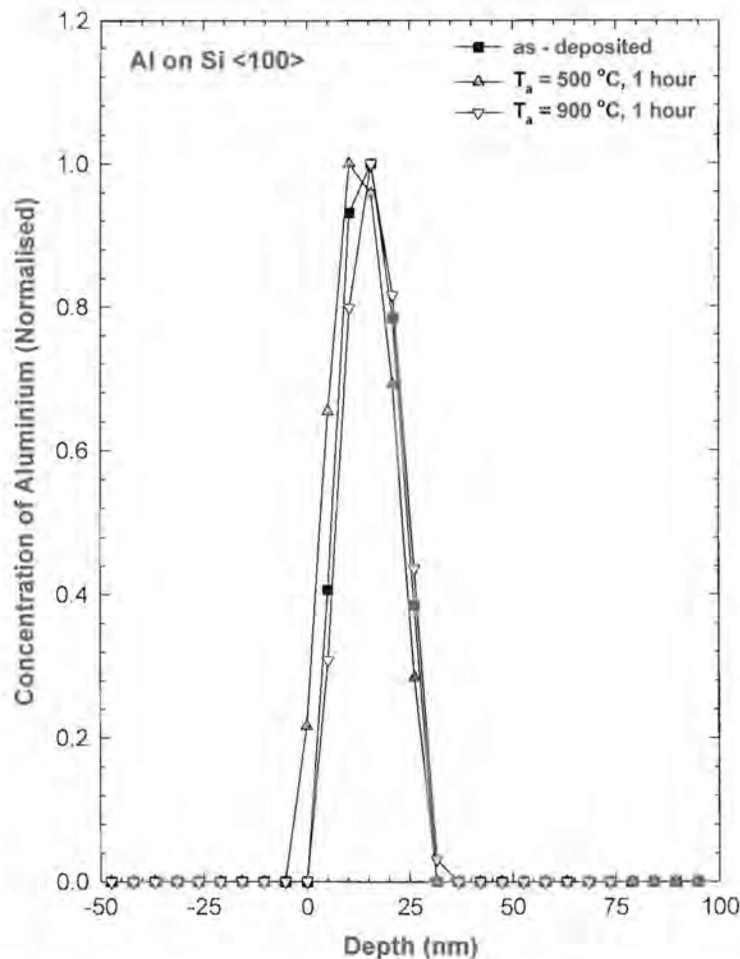

Fig. 19: Depth profiles of a vapour deposited aluminium film on Si <100> before and after annealing for one hour at different temperatures T_a.

The depth profiles of the deposited aluminium film before and after annealing for one hour at T_a = 500 and 900 °C respectively are shown in Fig. 19. The depth profiles, obtained with NRA, were corrected for proton straggling and energy resolution. A difference in the film thickness at the detection limit for our method at $\Delta d \approx 4$ *nm* was observed for T_a = 500 °C,

which is probably due to slight inhomogeneities when vapour depositing the aluminium film laterally onto the silicon wafer. However, it must be stressed that the film thickness does not contain information about in-diffusion.

If a detectable aluminium in-diffusion had occurred after annealing, the width of the interface between the aluminium film and the silicon substrate would increase. The interface width did not change within our detection limit and remained at 10 ± 4 *nm* before and after annealing at $T_a = 900$ °C. The aluminium in-diffusion at this temperature is below the detection limit for the applied method. An upper limit for the diffusion coefficient at $D \leq 10^{-16}$ $cm^2 s^{-1}$ for 900 °C was extracted from these results.

The data reported by other workers, which were obtained applying different techniques and at higher annealing temperatures were summarised in Fig. 17 and table 2 (page 47). An extrapolation of these data to 900 °C results in a diffusion coefficient between $D = 1.3 \times 10^{-13}$ $cm^2 s^{-1}$ and $D = 3 \times 10^{-15}$ $cm^2 s^{-1}$, which is at least an order of magnitude higher than the results obtained in this work.

However, the extracted limit for our diffusion coefficient might be too small due to a native oxide layer at the interface that forms instantaneously after cleaning the silicon surface before depositing of the aluminium film. This oxide layer is a diffusion barrier for the aluminium atoms. In order to avoid such an oxide layer, aluminium ions were implanted into a certain depth to be in direct contact with silicon.

7.1.2. ROOM TEMPERATURE IMPLANTATION

The implantation of 5×10^{16} aluminium ions cm^{-2} into Si <100> and Si <111> at room temperature created an amorphous layer in the surface region with thicknesses of $X_a = 376 \pm 19$ *nm* and $X_a = 367 \pm 19$ *nm* respectively, as deduced from the channeling spectra in Fig. 20, Fig. 21 and summarised in table 3. Partial regrowth of the crystal lattice from the bulk after annealing at $T_a = 500$, 700 and 900 °C was observed.

UNIVERSITEIT VAN PRETORIA
UNIVERSITY OF PRETORIA
YUNIBESITHI YA PRETORIA

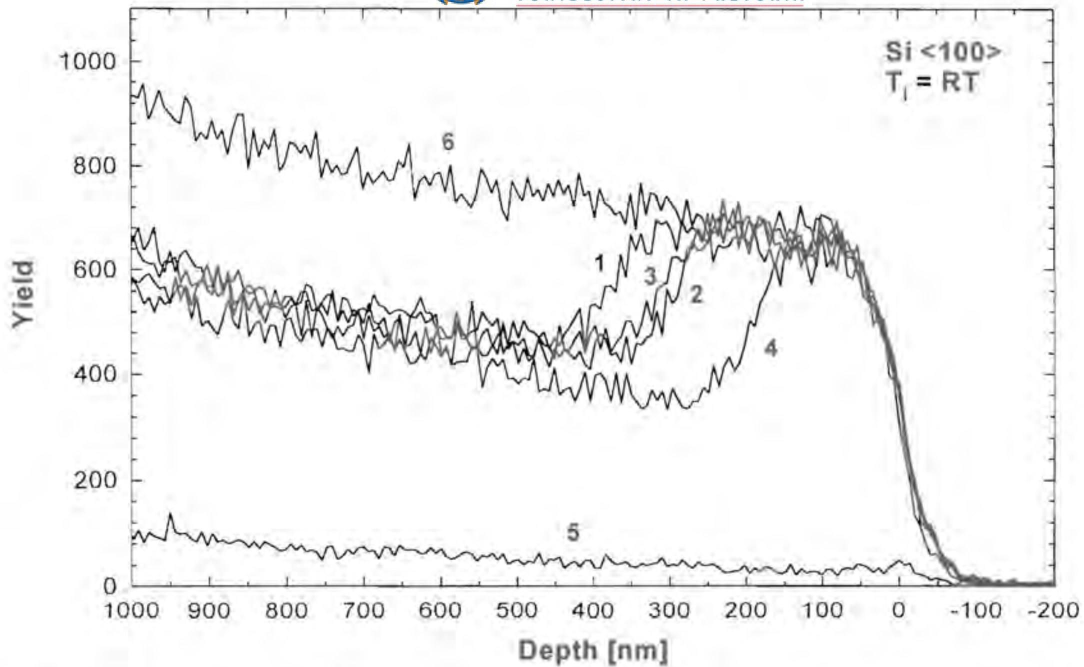

Fig. 20: Aligned backscattering spectra of Si <100> for room temperature implantation of 5 x 10^{16} Al^+ cm^{-2} before (1) and after annealing for one hour at 500 °C (2), 700 °C (3) and 900 °C (4). Also given are aligned (5) and random (6) spectra of unimplanted samples; α - particle energies have been converted to a depth scale.

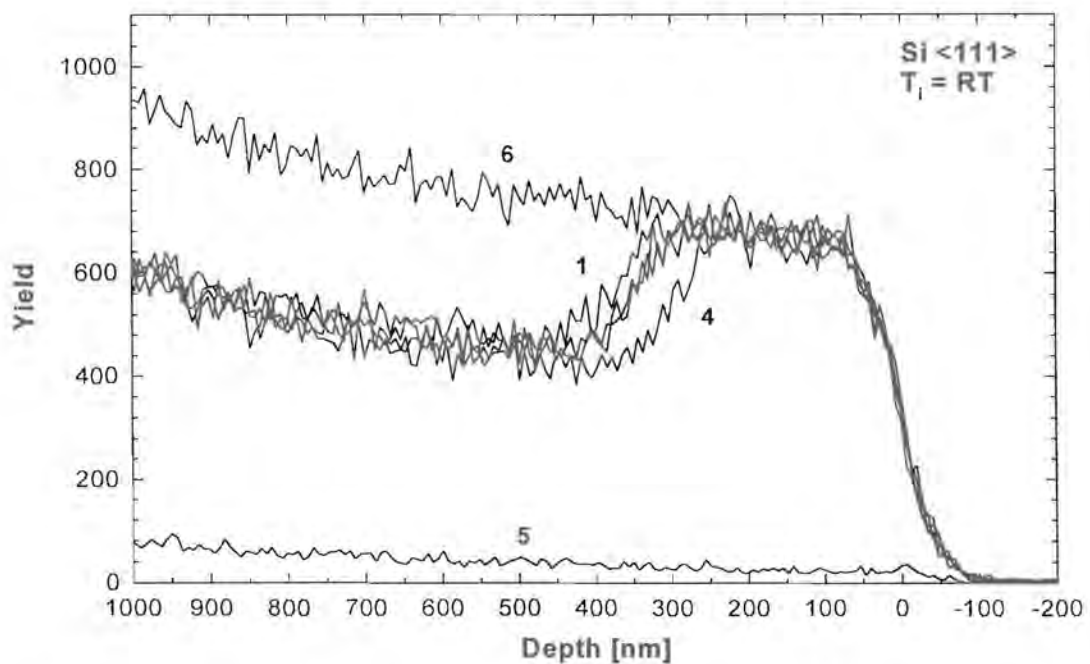

Fig. 21: Aligned backscattering spectra of Si <111> for room temperature implantation of 5 x 10^{16} Al^+ cm^{-2} before (1) and after annealing for one hour at 500 °C, 700 °C and 900 °C (4). Also given are aligned (5) and random (6) spectra of unimplanted samples; α - particle energies have been converted to a depth scale.

The amorphised surface layer of the Si <100> sample reduced to $X_a = 295 \pm 15$ *nm* during annealing at $T_a = 500$ °C. Within experimental uncertainty a similar thickness of the amorphous layer was found after annealing at $T_a = 700$ °C. However, during annealing at $T_a =$ 900 °C the thickness of the amorphous layer decreased further to $X_a = 197 \pm 11$ *nm* (Fig.20). For the Si <111> samples a significantly smaller crystalline regrowth was observed. The thickness of the amorphous layer reduced to $X_a = 349 \pm 18$ *nm* during annealing at $T_a = 500$ °C. A similar result within experimental uncertainty was obtained for the sample annealed at $T_a = 700$ °C, while the thickness of the amorphous layer decreased further to $X_a = 295 \pm 15$ *nm* after annealing at $T_a = 900$ °C (Fig. 21).

The apparent difference in annealing behaviour of the two lattice orientations might be explained by assuming that regrowth takes place along the preferred <100> direction. The experimentally observed ratio of $\Delta_{<111>} / \Delta_{<100>} = 0.40 \pm 0.14$ for the regrown layer thicknesses at 900 °C is just outside the 1σ error of the expected ratio of 0.58.

Sample	Thickness of highly disordered surface region X_a [*nm*]
Si <100> implanted at RT as implanted	376 ± 19
Annealed at 500 °C for 1 hour	295 ± 15
Annealed at 700 °C for 1 hour	308 ± 16
Annealed at 900 °C for 1 hour	197 ± 11
Si <111> implanted at RT as implanted	367 ± 19
Annealed at 500 °C for 1 hour	349 ± 18
Annealed at 700 °C for 1 hour	346 ± 18
Annealed at 900 °C for 1 hour	295 ± 15

Table 3: Thickness of the highly disordered surface region in silicon after aluminium implantation obtained with channeling.

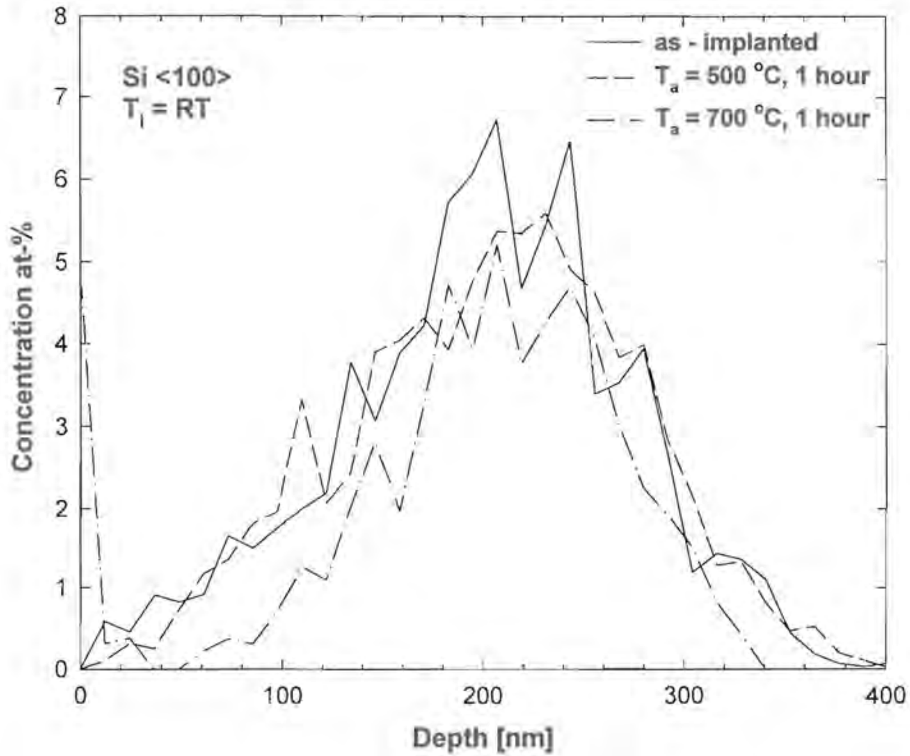

Fig. 22: Depth profiles of aluminium implanted at room temperature with a fluence of 5 x 10^{16} cm^{-2} into Si <100> before and after annealing for one hour at different temperatures.

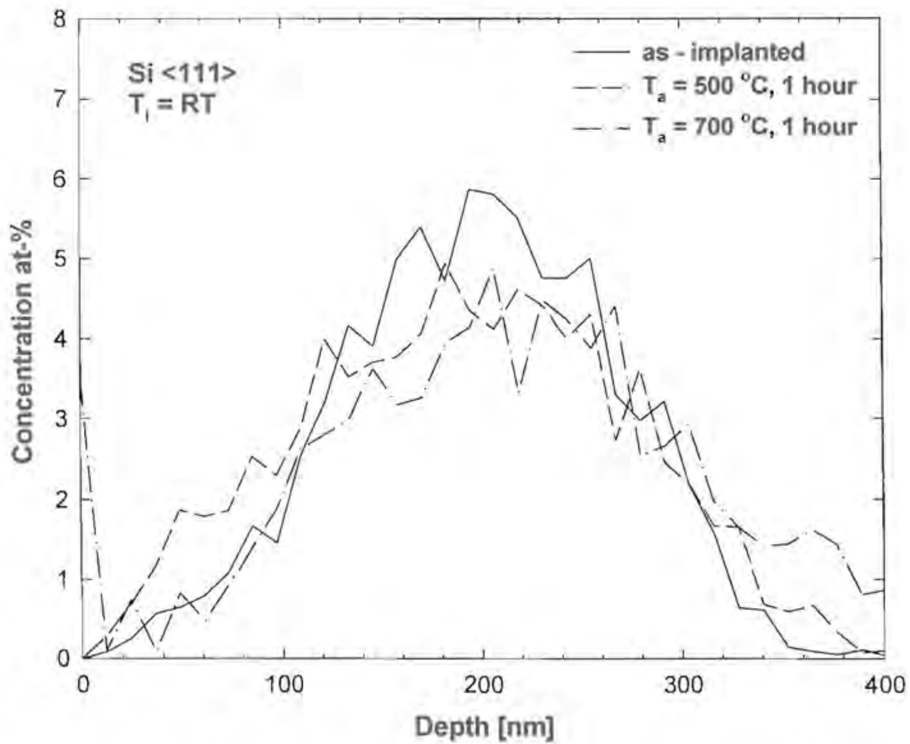

Fig. 23: Depth profiles of aluminium implanted at room temperature with a fluence of 5 x 10^{16} cm^{-2} into Si <111> before and after annealing for one hour at different temperatures.

The depth profiles of the implanted aluminium atoms before and after different annealing cycles are displayed in Fig. 22 and Fig. 23. The experimentally obtained mean ranges of the aluminium atoms were $R_p = 200 \pm 16$ *nm* in Si <100> and $R_p = 204 \pm 16$ *nm* in Si <111> before annealing.

Results for the second range moments were $\Delta R_p = 75 \pm 5$ *nm* for Si <100> and $\Delta R_p = 69 \pm 5$ *nm* for Si <111>. During annealing for one hour at $T_a = 500$ °C the second range moment stayed within experimental uncertainty at $\Delta R_p = 74 \pm 6$ *nm* in Si <100> and increased slightly to $\Delta R_p = 80 \pm 7$ *nm* in Si <111>. From these values aluminium diffusion coefficients below the detection limit of $D \leq 10^{-15}\ cm^2\ s^{-1}$ were obtained for both orientations.

After annealing for one hour at $T_a = 700$ °C an aluminium surface peak appears. However, the first range moment of the remaining implantation profile does not differ significantly from the as-implanted distribution for both orientations. The second range moment is slightly smaller but still within the experimental error. Apparently a small percentage of the aluminium starts at this temperature to diffuse to the surface, where it is trapped after reducing the native silicon oxide layer SiO_2 [63,65]. The temperature increase from 500 to 700 °C is not high enough to further improve the crystalline re-growth. The thickness of the amorphous surface layer is unchanged compared with the one at $T_a = 500$ °C. However, $T_a = 700$ °C is high enough to activate aluminium diffusion through the highly disordered region to the surface.

During annealing at $T_a = 900$ °C the implanted aluminium atoms diffused completely out of the sample to the surface. The damage depth is strongly reduced, however, the anomalous diffusion with coefficients of $D \approx 10^{-13}\ cm^2\ s^{-1}$ in both sample orientations is obviously due to defect structures still present after annealing at $T_a = 900$ °C and cannot be compared with aluminium diffusion coefficients in a defect-free silicon lattice.

7.1.3. HOT IMPLANTATION

The channeling spectra for Si <100> and Si <111> after implantation of 5 x 10^{16} aluminium ions cm^{-2} at $T_i = 250$ °C are displayed in Fig. 24 and Fig. 25. In both samples a surface region up to a depth of $X_c = 110 \pm 6$ *nm* was observed to be nearly defect-free.

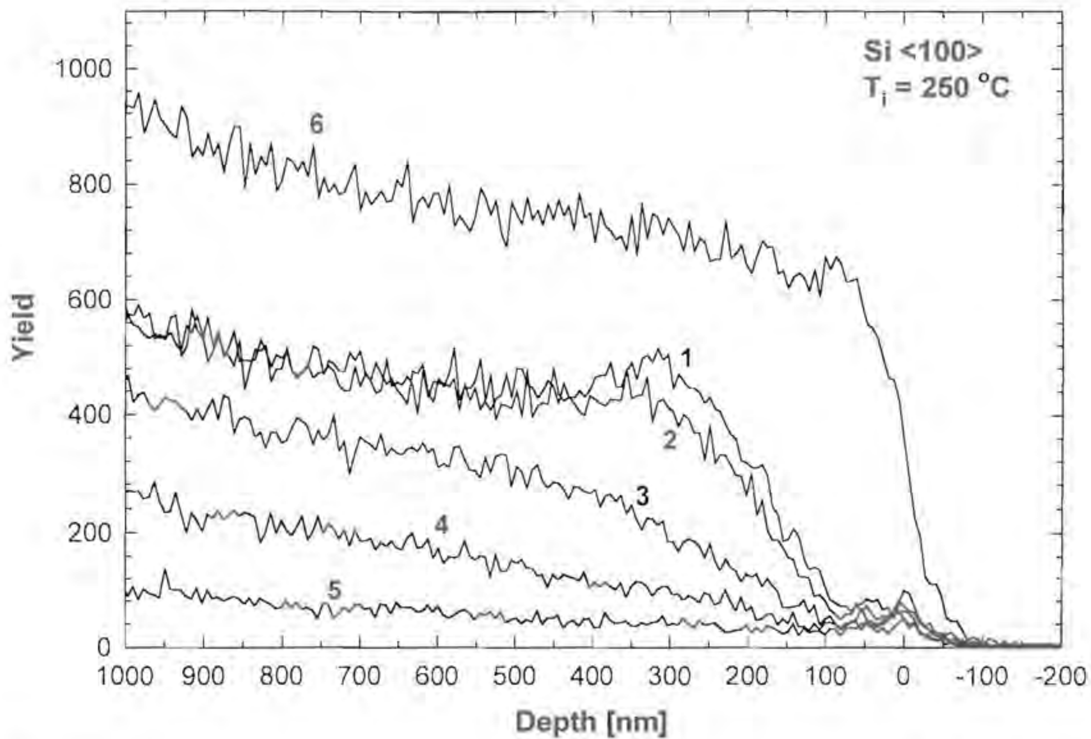

Fig. 24: Aligned backscattering spectra of Si <100> for implantation of 5 x 10^{16} Al^+ cm^{-2} at T_i = 250 °C before (1) and after annealing for one hour at 500 °C (2), 700 °C (3) and 900 °C (4). Also given are aligned (5) and random (6) spectra of unimplanted samples; α - particle energies have been converted to a depth scale.

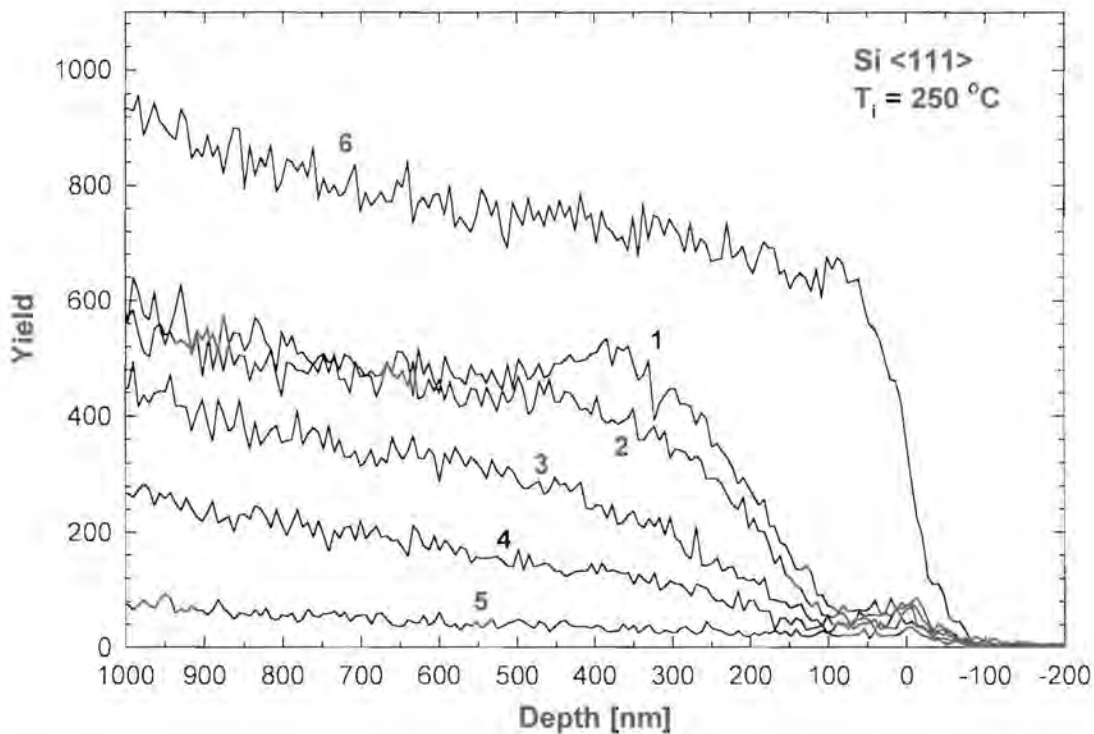

Fig. 25: Aligned backscattering spectra of Si <111> for implantation of 5 x 10^{16} Al^+ cm^{-2} at T_i = 250 °C before (1) and after annealing for one hour at 500 °C (2), 700 °C (3) and 900 °C (4). Also given are aligned (5) and random (6) spectra of unimplanted samples; α - particle energies have been converted to a depth scale.

Extended defect creation is prevented by irradiation induced annealing. No amorphous layer, as in the case of the room temperature implantation, was formed. The observed minimum yield in the region beyond the surface peak of the as-implanted Si<100> is χ_{min} = 14 %. After annealing at T_a = 500 °C the minimum yield reduced to χ_{min} = 9.8 % and to χ_{min} = 7 % after annealing at T_a = 700 °C. One hour of annealing at T_a = 900 °C resulted in a minimum yield of χ_{min} = 5.9 %. A similar behaviour was observed in Si <111>. Before annealing a minimum yield of χ_{min} = 14 % was obtained. The minimum yield improved to χ_{min} = 9.8 % after annealing at T_a = 500 °C and after annealing at T_a = 700 and 900 °C it was reduced to χ_{min} = 5.5 %.

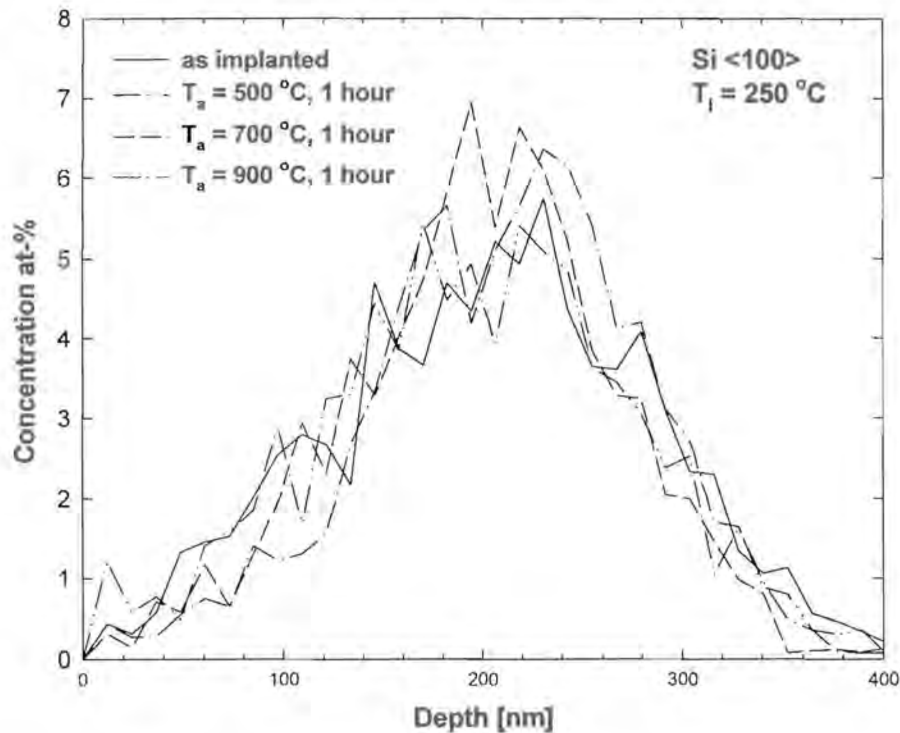

Fig. 26: Depth profiles of aluminium implanted at T_i = 250 °C with a fluence of 5 x 10^{16} cm^{-2} into Si <100> before and after annealing for one hour at different temperatures T_a.

In contrast to the room temperature implantation no significant difference is observed for the <100> and <111> orientation and strong annealing occurs between 500 and 700 °C. This is an indication that different radiation induced defects occur in the implanted depth compared to the room temperature implantation where complete amorphisation in the surface region up to and slightly beyond the implanted depth was observed.

From the reduction of the dechanneling yield it is obvious that the dislocation density reduces during each annealing temperature. The values for the minimum yield obtained after annealing at T_a = 900 °C were only slightly higher than those of unimplanted samples prepared from the same wafers. The χ_{min} of virgin Si <100> was at 4.4 % slightly higher than that of Si <111> at 3.7 %. From the shape of the channeling spectra and the low minimum yield it can be concluded that radiation induced annealing plays an important role during implantation at T_i = 250 °C.

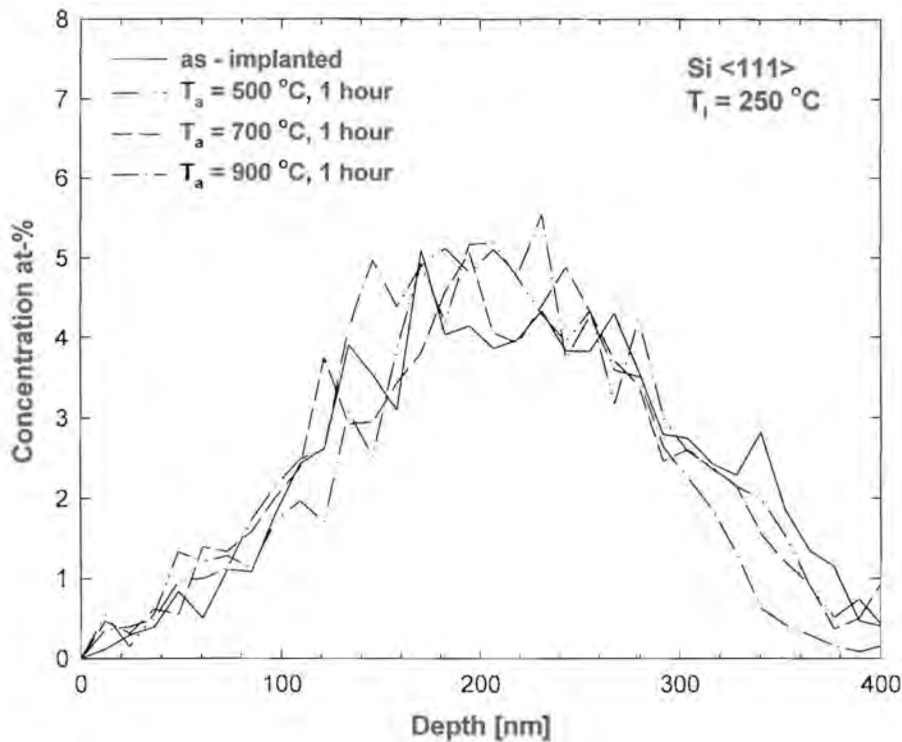

Fig. 27: Depth profiles of aluminium implanted at T_i = 250 °C with a fluence of 5 x 10^{16} cm^{-2} into Si <111> before and after annealing for one hour at different temperatures T_a.

The depth profiles of aluminium in Si <100> and Si <111> after the hot implantation are displayed in Fig. 26 and Fig. 27, respectively. Annealing at temperatures of T_a = 500, 700 and 900 °C for one hour does not change the shape of the implanted aluminium depth profile significantly. The mean projected range of the as-implanted aluminium is $R_p = 204 \pm 16$ *nm* in Si <100> and $R_p = 220 \pm 16$ *nm* in Si <111>. The values obtained for the second range moment are $\Delta R_p = 79 \pm 6$ *nm* and $\Delta R_p = 83 \pm 7$ *nm*, respectively. These values agree within experimental error with those obtained for the room temperature implantation before

annealing. For our hot implantation parameters radiation enhanced diffusion coefficients below the detection limit at $D \leq 10^{-15}$ cm^2 s^{-1} were obtained for both orientations by taking into account the implantation time. In Si <100> the mean projected range stays constant within experimental error during annealing for one hour at T_a = 900 °C. The value obtained for the second range moment stayed constant up to an annealing temperature of T_a = 700 °C. It decreased slightly to ΔR_p = 68 ± 5 *nm* during annealing at T_a = 900 °C, but was still within the experimental error.

Sample	**Range** R_p [*nm*]	**Second moment** ΔR_p [*nm*]	**Thermal diffusion Coefficient** D [cm^2 s^{-1}]
Si (100), $T_i = RT$	200 ± 16	75 ± 5	-
T_a = 500 °C, 1 hour	206 ± 16	74 ± 6	$\leq 10^{-15}$
T_a = 700 °C, 1 hour	210 ± 16	65 ± 5	(*) $\approx 10^{-15}$
T_a = 900 °C, 1 hour	Complete out-diffusion to the surface		(*) $\approx 10^{-13}$
Si (100), T_i = 250 °C	204 ± 16	79 ± 6	-
T_a = 500 °C, 1 hour	196 ± 16	78 ± 6	$\leq 10^{-15}$
T_a = 700 °C, 1 hour	199 ± 16	67 ± 5	$\leq 10^{-15}$
T_a = 900 °C, 1 hour	212 ± 16	68 ± 5	$\leq 10^{-15}$
Si (111), $T_i = RT$	204 ± 16	69 ± 5	-
T_a = 500 °C, 1 hour	204 ± 16	80 ± 6	$\leq 10^{-15}$
T_a = 700 °C, 1 hour	223 ± 16	76 ± 7	(*) $\approx 10^{-15}$
T_a = 900 °C, 1 hour	Complete out-diffusion to the surface		(*) $\approx 10^{-13}$
Si (111), T_i = 250 °C	220 ± 16	83 ± 7	-
T_a = 500 °C, 1 hour	215 ± 16	82 ± 7	$\leq 10^{-15}$
T_a = 700 °C, 1 hour	212 ± 16	83 ± 7	$\leq 10^{-15}$
T_a = 900 °C, 1 hour	200 ± 16	73 ± 6	$\leq 10^{-15}$

Table 4: Range parameters and thermal diffusion coefficients of implanted aluminium in silicon obtained with NRA.

A similar behaviour is observed in Si <111>. Here the second moment stayed constant up to an annealing temperature of T_a = 700 °C. It decreased slightly to ΔR_p = 73 ± 6 *nm* during annealing at T_a = 900 °C. A summary of the experimental range moments and diffusion coefficients is shown in table 4. The diffusion coefficients marked with (*) are defect induced and several orders of magnitude larger than those expected in defect free silicon.

The dechanneling yield in the aligned spectrum of the as-implanted sample reaches a maximum between 350 and 380 *nm* into the crystal, which is much deeper than the mean range of the implanted aluminium ions.

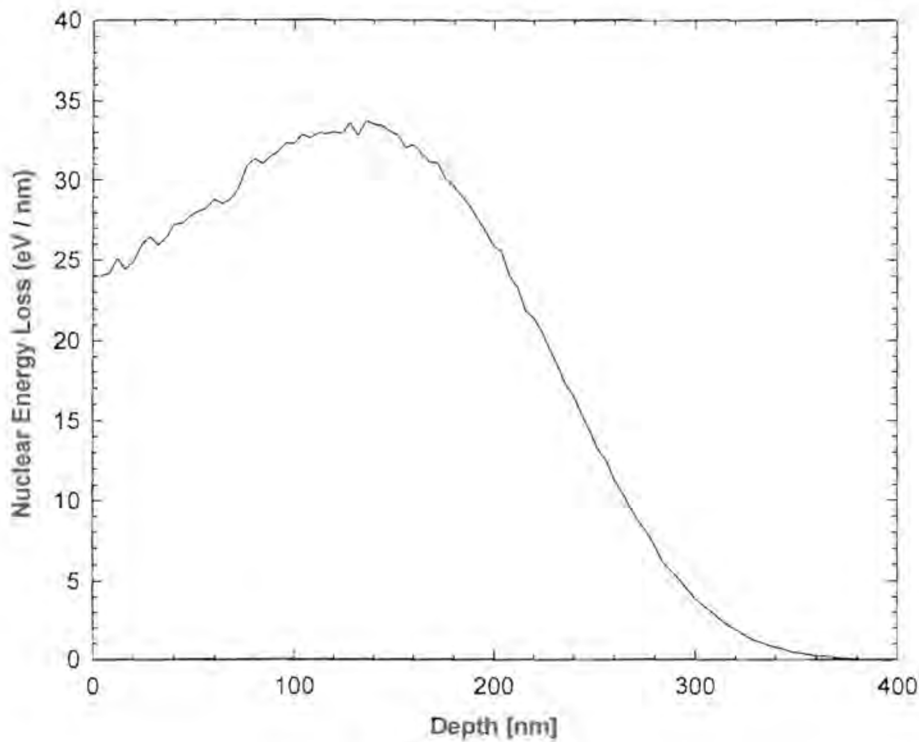

Fig. 28: TRIM calculation of the nuclear energy loss for an aluminium ion in silicon at an energy of 120 keV.

The nuclear energy loss depth distribution from an aluminium implantation at an energy of 120 *keV* calculated by TRIM (SRIM 2000 – Version) is displayed in Fig. 28. This nuclear energy loss was obtained by adding the energy losses due to recoil collisions and phonon creation. The radiation-induced damage in the target is closely related to this nuclear energy loss. From this calculation it is therefore deduced that the damage range, which is defined as the distance from the surface at which the defect density drops to 50 % of its maximum, is at

a depth of 243 *nm*. However, the experimentally observed damage reaches about 100 *nm* deeper into the crystal than the predicted nuclear energy loss. Such enhanced damage ranges were previously only reported in metals [93], where they could be explained with the formation of dislocations reaching much deeper than the mean range of the implanted ions.

The damage peaks disappear during annealing and the remaining slopes of the dechanneling yield near the surface for T_a = 900 °C is not much larger than for unimplanted samples. The slightly higher dechanneling slope beyond a depth of approximately 100 *nm* is due to the implanted aluminium, which reaches a peak concentration of about 5 at.% at 200 *nm*. No channeling effect was, however, observed for the γ-ray yield with a proton beam, indicating random lattice positions for the impurity atoms. This is expected because of the extremely low solubility of aluminium in silicon [55].

The dramatic change of the aligned spectra for α-particles during annealing, without a corresponding change of the implantation profiles can only be explained by assuming that during the hot implantation an amorphisation of the target is effectively prevented. Only short-range disorder appears to occur near the end of the ion range with most of the lattice information still available to allow complete re-growth during annealing.

From the binary phase diagram [55] for the silicon aluminium system it is obvious, that for a maximum concentration of about 5 at.% aluminium at a target depth of 200 *nm* two phases are formed at 900 °C. At this depth 8 % of the compound will be in the liquid phase, consisting of 37 % silicon and 63 % aluminium. The solid phase mainly consists of silicon due to the low solubility of aluminium. When cooling the samples after annealing, aluminium probably segregates at its implanted depth.

An Arrhenius plot of previously reported aluminium diffusion coefficients in silicon, including the results obtained in this study is displayed in Fig. 29. An upper limit for the diffusion coefficients at $D \leq 10^{-15}$ cm^2 s^{-1} was extracted after annealing samples of the hot implantation. Our diffusion coefficients are about an order of magnitude smaller than the values obtained by extrapolating previously published results to 900 °C and could be explained by segregation into metallic aluminium during annealing [64]. The value from the

room temperature implantation is much too high, due to defect assisted diffusion, but corresponds well with some of the published values. The upper limit from the in-diffusion investigation $D \leq 10^{-16}$ $cm^2\ s^{-1}$ at 900 °C is also included in this figure. However, this limit is probably too low due to the native silicon oxide layer at the interface.

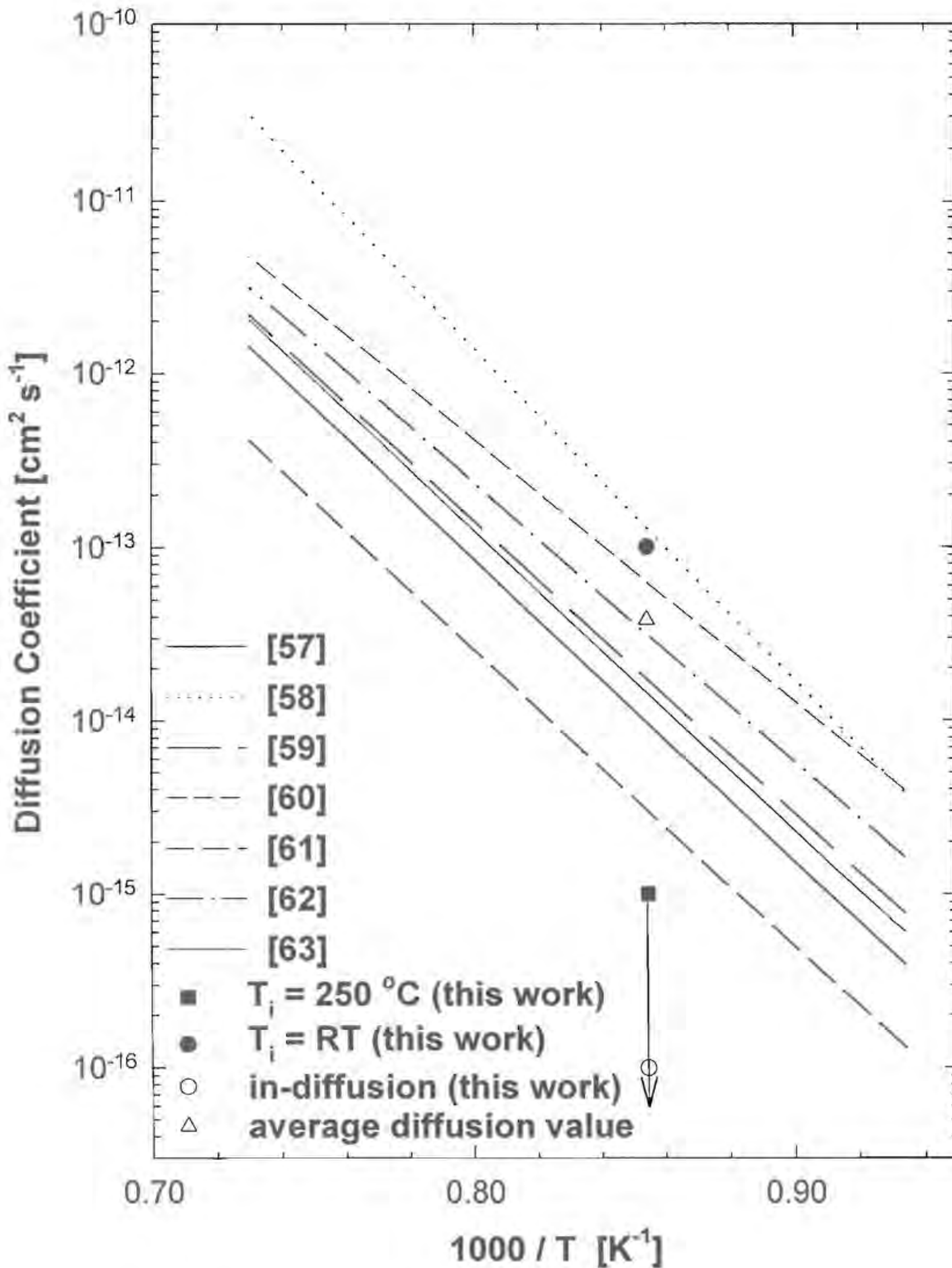

Fig.29: Comparison of the diffusion coefficients of aluminium in silicon obtained in this work at 900 °C with previously reported results (table 2).

7.2. GERMANIUM

In comparison with silicon relatively little research was done on germanium in recent years. To our knowledge only two investigations on aluminium diffusion in germanium were reported previously. One of them dating back to 1982 by *Dorner* et al. [71], the other to 1967 by *Meer* et al.[72]. From the results by *Meer* et al. expected diffusion coefficients are calculated to $D = 1 \times 10^{-19}\ cm^2\ s^{-1}$ and $D = 2.4 \times 10^{-15}\ cm^2\ s^{-1}$ at 500 °C and 700 °C, respectively. *Dorner* et al. measured a diffusion coefficient of $D = 1.2 \times 10^{-15}\ cm^2\ s^{-1}$ at 700 °C. After extrapolating their results to 500 °C a coefficient of $D = 3 \times 10^{-20}\ cm^2\ s^{-1}$ is calculated. As these are the only two reports on aluminium diffusion in germanium and their results differ by factors of 2-3, the present study was performed to verify the validity of these results by applying a different analysing method. At 700 °C the aluminium diffusion coefficients appear to be in the range that can be detected with our analysing method.

7.2.1. ALUMINIUM DIFFUSION INTO GERMANIUM

The in-diffusion of aluminium into <111> germanium for temperatures up to 700 °C was investigated. A thin aluminium film was deposited onto clean crystalline germanium. The deposited amount of aluminium is crucial [71]. It should not be too large because of its low solubility in germanium and due to its high vapour pressure at the selected annealing temperatures it can partly vaporise from the surface. Ideal film thicknesses for in-diffusion analysis were experimentally determined to be between 5 and 28 *nm* [71]. The thickness of our deposited aluminium film at 13 ± 3 *nm* is within this interval.

The samples cut from this wafer were analysed before and after the different annealing cycles. The normalised depth profiles of the aluminium films before and after annealing for 1 hour at $T_a = 500$ °C and $T_a = 700$ °C, respectively are shown in Fig. 30.

Slight differences in the film thickness of $\Delta d \approx 4\ nm$ just at the detection limit are due to inhomogeneities during the lateral vapour deposition onto the wafer. However, the film thickness holds no diffusion information and such small differences are actually below the detection limit of our system.

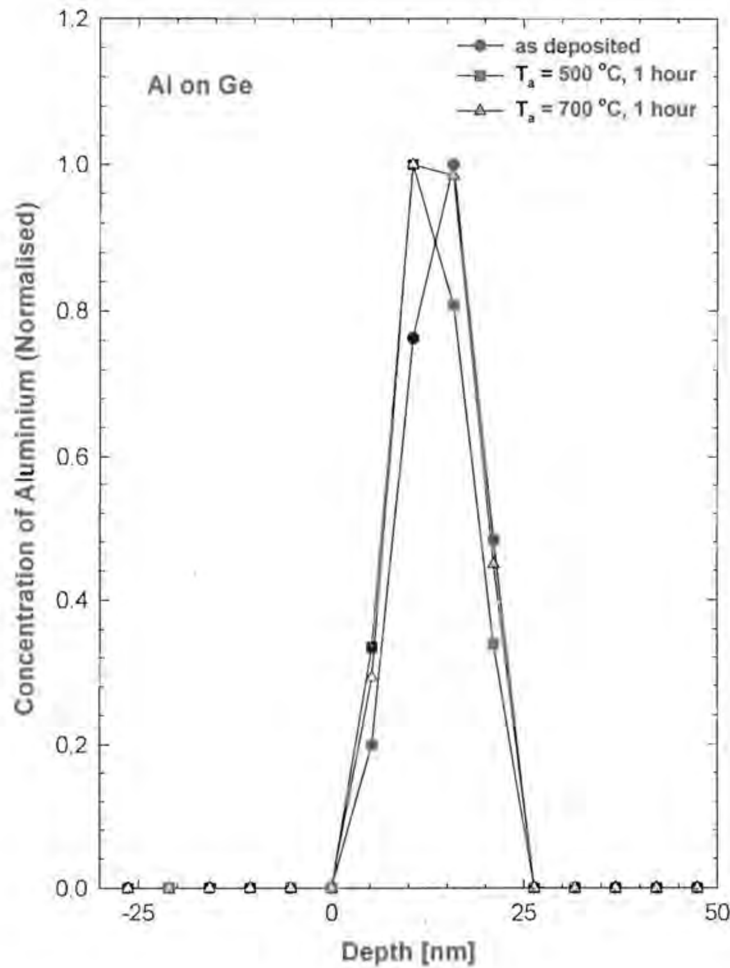

Fig. 30: Depth profiles of a vapour deposited aluminium layer on germanium before and after annealing for one hour at different temperatures T_a.

The width of the interface between the aluminium film and the germanium bulk material remains within experimental error at 5 *nm* before and after annealing for one hour at $T_a = 700$ °C. Therefore no significant aluminium diffusion into the germanium sample occurred. An upper limit for the diffusion coefficient at $D \leq 10^{-16}$ cm^2 s^{-1} for 500 and 700 °C was extracted from the aluminium depth profiles.

In the case of 500 °C the diffusion coefficient obtained in this study did not contradict the predicted values by *Dorner* and *Meer*. However, the upper limit for the diffusion coefficient of $D \leq 10^{-16}$ cm^2 s^{-1} extracted after annealing for one hour at $T_a = 700$ °C is an order of magnitude lower than the ones expected from *Dorner* and *Meer*.

A thin native oxide layer forms instantaneously after cleaning the germanium substrate due to the low heat of formation for this reaction. This oxide layer can act as a diffusion barrier for the aluminium atoms. The obtained upper limit of the diffusion coefficients is therefore probably too small. Additional measurements on this system were performed, where the diffusion source was placed within the germanium by aluminium ion implantation. This brings the two elements into direct contact with each other.

7.2.2. ROOM TEMPERATURE IMPLANTATION

The depth profiles of 5×10^{16} aluminium ions cm^{-2} implanted into germanium at room temperature before and after subsequent annealing for one hour at T_a = 500 and 700 °C are shown in Fig. 31. The experimentally obtained mean range of the implanted aluminium ions before annealing was at $R_p = 107 \pm 13$ nm with a second range moment of $\Delta R_p = 53 \pm 4$ nm. After annealing at T_a = 500 °C for one hour the mean range of the aluminium atoms in the germanium reduced to $R_p = 82 \pm 13$ nm which is just within experimental error of the value before annealing. However, the depth profile becomes also wider and changes dramatically. The second range moment $\Delta R_p = 86 \pm 6$ nm is outside the experimental error. Diffusion out of the sample to the surface occurred. The observed high aluminium concentration at the surface together with its high affinity for oxygen leads to the suspicion that Al_2O_3 segregates at the surface. An aluminium diffusion coefficient of $D \approx 10^{-14}$ $cm^2\,s^{-1}$ was extracted at T_a = 500 °C.

Annealing for one hour at T_a = 700 °C caused a large fraction of aluminium atoms to diffuse out of the sample to the surface. The mean range and the second range moment of the remaining aluminium atoms in the sample were at $R_p = 117 \pm 25$ nm and $\Delta R_p = 56 \pm 15$ nm, respectively, and therefore within experimental error of the range parameters before annealing. However, the remaining maximum aluminium concentration within the target was 1.5 at. %, which was much lower than the maximum concentration of 8 at. % before annealing. A diffusion coefficient of $D \approx 10^{-13}$ $cm^2\,s^{-1}$ at 700 °C was extracted for aluminium in germanium.

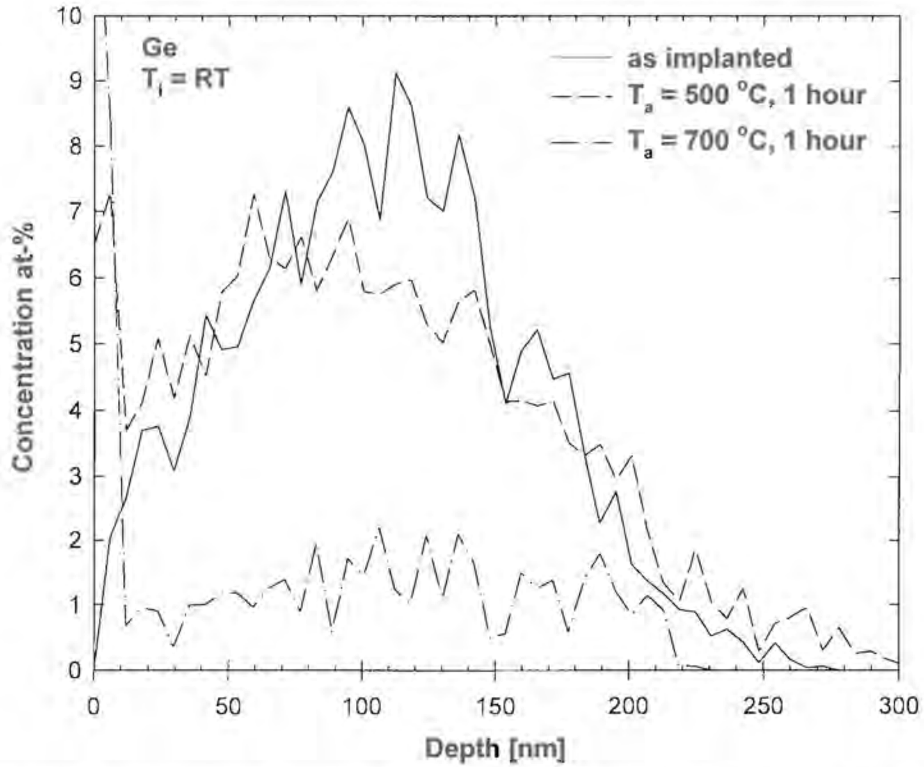

Fig. 31: Depth profiles of aluminium implanted at room temperature into germanium before and after annealing for one hour at different temperatures T_a.

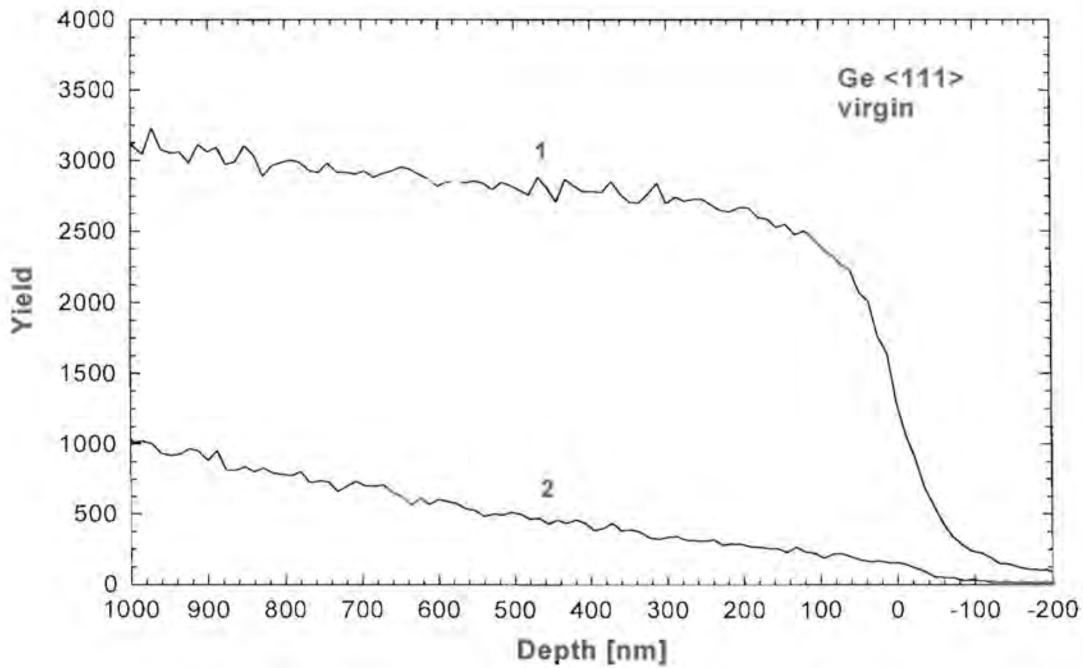

Fig. 32: Random (1) and aligned (2) backscattering spectra of Ge<111> before implantation.

The channeling spectra for a Ge<111> sample before implantation is displayed in Fig. 32. The minimum yield of the aligned spectrum is χ_{min} = 15 % and a rather high dechanneling yield is observed. No change in the dechanneling behaviour was observed after annealing the unimplanted germanium sample for two hours at T_a = 600 °C. This is an indication that extended defects such as dislocations are present deep into the crystal. Channeling spectra of implanted samples could not be obtained due to the heavy radiation-induced damage in samples with an already high defect concentration. A hot implant largely avoids this damage but those channeling spectra could also not be obtained because of the large scattering cross section of displaced germanium atoms.

Due to radiation induced damage in germanium the aluminium diffusion appears to be largely enhanced. This effect was also observed for the room temperature implanted silicon (chapter 7.1.) and the extracted diffusion coefficients are much too large if compared to those obtained from the aluminium in-diffusion experiments into germanium.

7.2.3. HOT IMPLANTATION

The same fluence of aluminium ions as for the room-temperature implantation was implanted at T_i = 250 °C into several germanium samples. The aluminium depth profiles before and after annealing for one hour at T_a = 500 and 700 °C respectively are displayed in Fig. 33.

The mean range of the aluminium atoms is at a depth of R_p = 111 ± 13 *nm* with a second range moment of ΔR_p= 59 ± 5 *nm*. These aluminium range moments in germanium agree within the experimental error with those obtained for the room temperature implantation. No noticeable difference is observed in the distribution. The upper limit for the radiation-enhanced diffusion during the hot implantation is therefore at $D \leq 10^{-15}$ cm^2 s^{-1} for our implantation parameters by taking into account the implantation time.

After annealing for one hour at T_a = 500 °C the mean range of the implanted aluminium atoms was measured at R_p = 106 ± 13 *nm* with a second range moment of ΔR_p= 54 ± 4 *nm*. The diffusion of aluminium atoms to the surface, which was observed after annealing the room-temperature implanted samples, did not occur after annealing the hot implants for one hour at T_a = 500 °C. An upper limit for the diffusion coefficient of $D \leq 10^{-15}$ cm^2 s^{-1} at 500 °C

was extracted, which does not contradict the predicted coefficients from *Dorner* [71] and *Meer* [72] as those are much smaller and not measurable with our method.

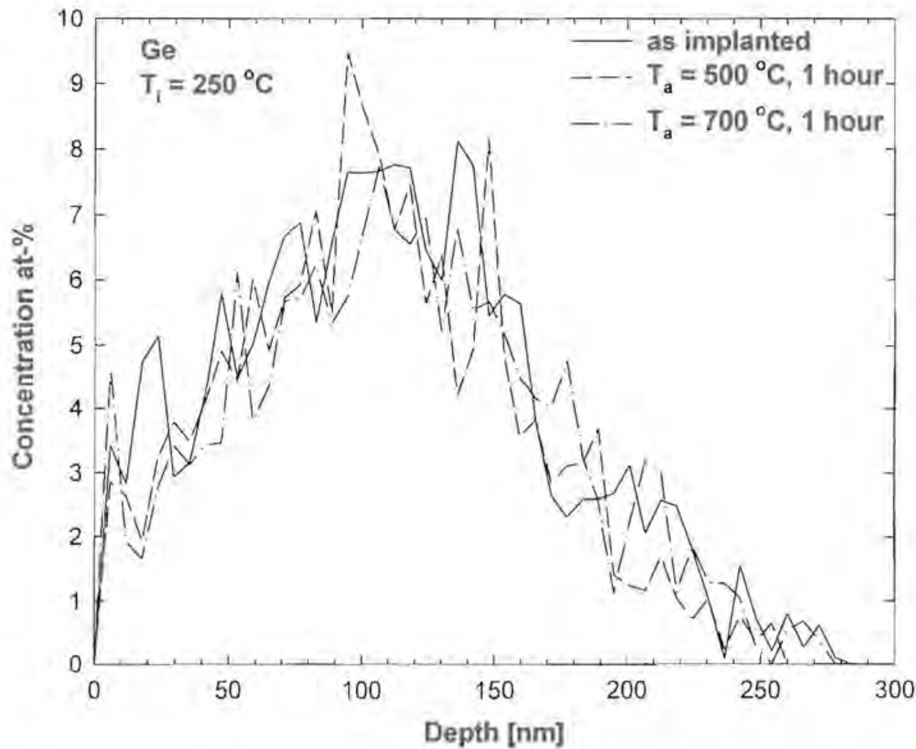

Fig. 33: Depth profiles of aluminium implanted at T_i = 250 °C with a fluence of 5 x 10^{16} cm^{-2} into germanium before and after annealing for one hour at different temperatures T_a.

Annealing for one hour at T_a = 700 °C results in a mean range of the implanted aluminium atoms of R_p = 115 ± 13 *nm* with a second range moment of ΔR_p = 59 ± 5 *nm*. These values agree within experimental error with those obtained before annealing. The upper limit for the diffusion coefficient is again at $D \leq 10^{-15}$ cm^2 s^{-1} and agrees with values obtained for the in-diffusion analysis. It is, however, smaller by a factor of two compared to the calculated coefficients from the data by *Meer* at 700 °C but does not contradict the experimental results by *Dorner*.

The maximum concentration of about 7 at.% aluminium in germanium is at a depth of 110 *nm*. For the germanium aluminium system it is obvious from the binary phase diagram [70], that at this depth two phases are formed at 700 °C. About 17 % of the compound are in the liquid phase, consisting of 57 % germanium and 43 % aluminium. The solid phase mainly consists of germanium due to the fairly low solubility of aluminium. When cooling the samples after annealing aluminium is suspected to segregate at the implanted depth.

An Arrhenius plot of the previously reported diffusion coefficients as well as the results obtained in this study is shown in Fig. 34. The rather small upper limit obtained from the in-diffusion analysis (hollow circle) is probably due to the native oxide layer at the interface between the aluminium film and the germanium substrate. A few monolayers of GeO_2 act as a diffusion barrier, which limits a possible aluminium in-diffusion. Diffusion coefficients obtained from the hot implantation agree well with results obtained by *Dorner*.

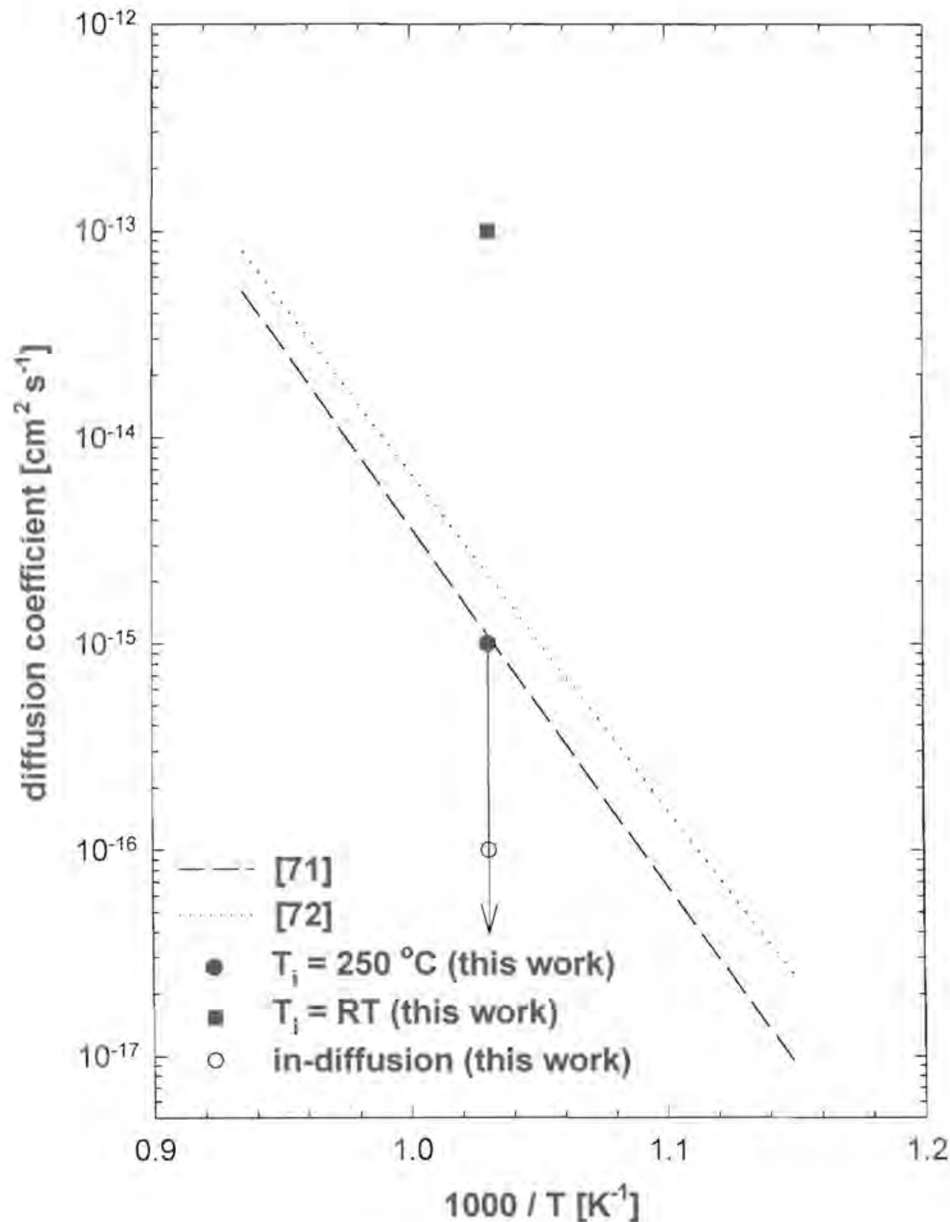

Fig. 34: Comparison of the diffusion coefficients of aluminium in germanium obtained in this work at 700 °C with previously reported results.

Sample Germanium	Range R_p [nm]	Straggling ΔR_p [nm]	Thermal diffusion coefficient D [$cm^2\,s^{-1}$]
T_I = RT, as-implanted	107 ± 13	53 ± 4	-
T_I = RT, T_a = 500 °C	82 ± 13	86 ± 6	(*) $\approx 10^{-14}$
T_I = RT, T_a = 700 °C	117 ± 25	56 ± 15	(*) $\approx 10^{-13}$
T_I = 250 °C, as implanted	111 ± 13	59 ± 5	-
T_I = 250 °C, T_a = 500 °C	106 ± 13	54 ± 4	$\leq 10^{-15}$
T_I = 250 °C, T_a = 700 °C	115 ± 13	59 ± 5	$\leq 10^{-15}$

Table 5: Range parameters of aluminium in germanium and thermal diffusion coefficients.

Table 5 summarises obtained range parameters of the implanted aluminium in germanium before and after annealing, as well as the upper limits for the diffusion coefficients at 500 °C and 700 °C. The coefficients marked with (*) are probably damage induced and some orders of magnitude larger than those expected in nearly defect free germanium. The observed aluminium out-diffusion after annealing the room-temperature implanted germanium is most probably due to the radiation induced disorder still present after annealing at T_a = 700 °C as no detectable aluminium diffusion occurred during annealing the hot implanted germanium samples at this temperature.

7.3. GALLIUM ARSENIDE

Gallium arsenide is a widely used compound semiconductor. Due to the possibility of the formation of superlattices many results on the inter-diffusion of aluminium and gallium were reported as described in chapter 6.2.1. It was found that the self-diffusion of gallium in gallium arsenide is strongly correlated to the aluminium diffusion in this compound.

For higher annealing temperatures it is necessary to supply the samples with an arsenic overpressure in order to avoid arsenic loss to the vapour phase. This already happens at temperatures in excess of $T_a \approx 600$ °C [81,89]. From the binary phase diagram [90] it is obvious that an arsenic loss of the compound at temperatures above $T > 29.7$ °C shifts the alloy to a two-phase region, where a small percentage, consisting mainly of gallium, would be in the liquid phase. A diffusion prediction is not possible for such a degraded compound. An arsenic loss has therefore to be avoided. Due to unavailability of a facility to anneal the samples at an arsenic overpressure, anneals in this study were performed at $T_a \leq 500$ °C to stay well below the critical temperature. As there was generally no difference between the experimental results for $T_a = 400$ °C and $T_a = 500$ °C, only results for the higher annealing temperature are given in this chapter.

When extrapolating Fig. 18, the diffusion coefficient at 500 °C is expected to be about $D \approx 10^{-30}$ cm^2 s^{-1} and therefore much lower than the detection limit of the applied method. However, the radiation-induced amorphisation in elemental semiconductors silicon and germanium after room temperature implantation, which is described in chapters 7.1. and 7.2., respectively, resulted in an enhancement of the aluminium diffusion coefficient by several orders of magnitude. This study of the GaAs-Al system was performed to investigate if radiation induced aluminium diffusion is observed. Results from annealing room temperature implanted samples, where a diffusion enhancement could be possible, are compared with those from the in-diffusion investigation and the hot implantation study.

7.3.1. ALUMINIUM DIFFUSION INTO GALLIUM ARSENIDE

The in-diffusion of aluminium into gallium arsenide at T_a = 500 °C was investigated. This investigation was performed to compare our results with previously reported diffusion coefficients that were mainly obtained by investigating inter-diffusion of multilayered structures (chapter 6.2.1.). A gallium arsenide wafer was cut in half and cleaned. Onto one of the halves a 17 ± 4 *nm* film of aluminium was deposited. Samples cut from this piece were analysed before and after different annealing cycles.

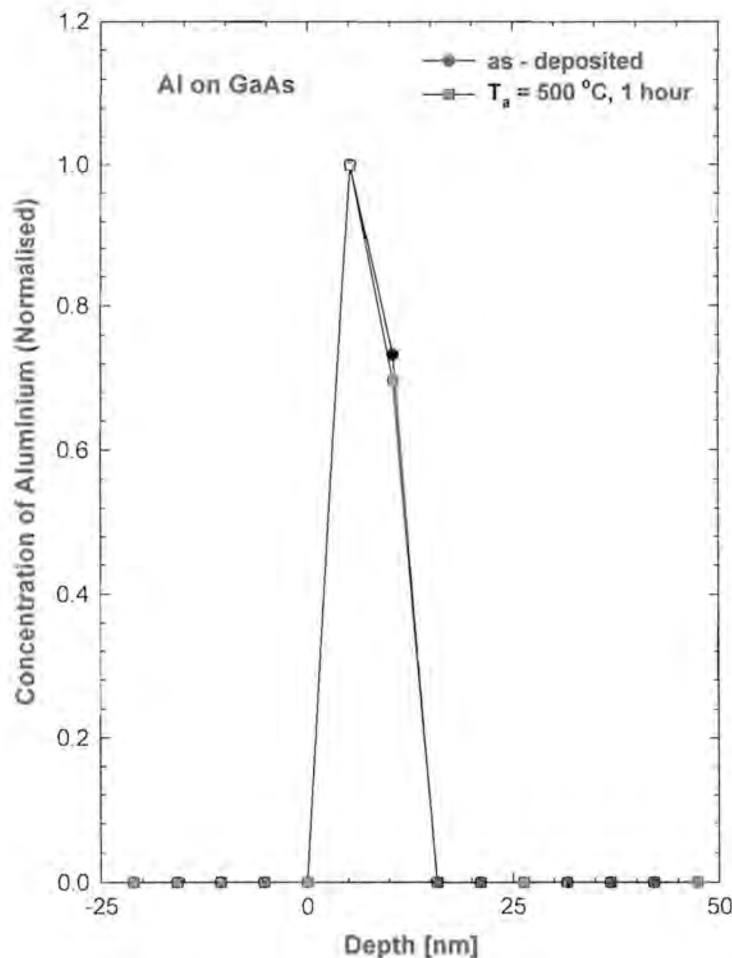

Fig. 35: Depth profiles of a vapour deposited aluminium layer on gallium arsenide before and after annealing for one hour at different temperatures T_a.

The depth profiles of the aluminium layer before and after annealing for one hour at T_a = 500 °C are shown in Fig. 35. The aluminium depth profile, measured after annealing another

sample for one hour at T_a = 400 °C, closely resembles the displayed profiles and is therefore not shown.

No variation in thickness of the aluminium films on gallium arsenide samples was observed from which it was concluded that the vapour deposition onto the gallium arsenide half was homogeneous. The width of the interface between the aluminium layer and the gallium arsenide sample stayed constant within experimental error at 5 *nm* before and after annealing at T_a = 500 °C for one hour, and no change in shape of the depth profiles was observed.

As the interface remains sharply defined up to the highest annealing temperature no significant aluminium in-diffusion into the gallium arsenide sample occurred. An upper limit for the diffusion coefficient of $D \leq 10^{-16}$ cm^2 s^{-1} at 500 °C was extracted from the aluminium depth profiles which was expected because of the predicted undetectable diffusion coefficient from previous investigations on inter-diffusion in multilayer-structures.

7.3.2. ROOM TEMPERATURE IMPLANTATION

Defect induced diffusion played an important role in the diffusion behaviour of the room temperature implanted elemental semiconductors. This study is to investigate if such an enhancement is also observed in gallium arsenide. The room temperature implantation of 5 x 10^{16} aluminium ions cm^{-2} into gallium arsenide created an amorphous region at the surface of the sample. Strong dechanneling prevents the channeling effect to be seen at larger depths even after annealing samples for one hour at T_a = 400 °C.

After annealing samples for one hour at T_a = 500 °C a highly disordered surface region still remains, however some of the introduced damage annealed out already at this temperature and a channeling effect was seen at larger depths, which is displayed in Fig. 36. This agrees with previously reviewed minimum temperatures for measurable regrowth, which was observed to occurs in the annealing behaviour of amorphised layers in *III-V* semiconductors at T_a = 500 °C [91]. The thickness of the disordered surface region in the sample is about X_a = 160 ± 20 *nm* and is therefore still slightly deeper than the mean range of the implanted aluminium atoms.

The depth profiles of 5 x 10^{16} aluminium ions cm^{-2} implanted into gallium arsenide at room temperature before and after annealing for one hour at T_a = 500 °C are shown in Fig. 37.
The experimentally obtained mean range of the implanted aluminium ions before annealing was $R_p = 152 \pm 16$ *nm* and the second range moment was $\Delta R_p = 66 \pm 5$ *nm*.

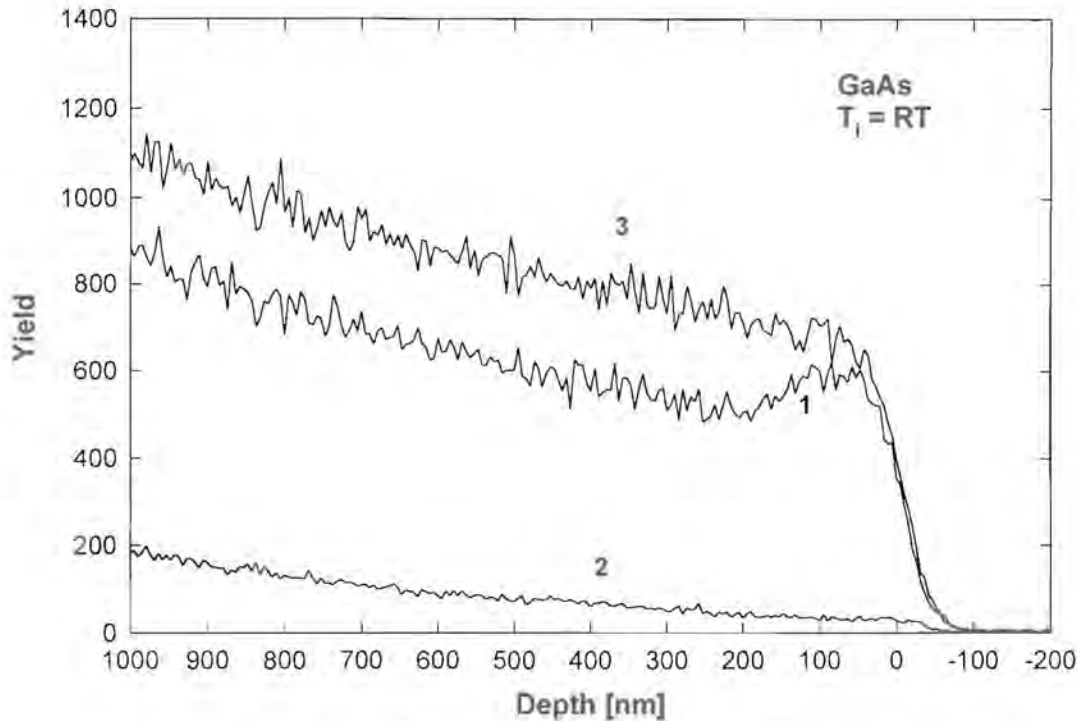

Fig. 36: Aligned backscattering spectra of gallium arsenide for room temperature implantation of 5 x 10^{16} Al^{+} cm^{-2} after annealing for one hour at 500 °C (1). Also given are aligned (2) and random (3) spectra of unimplanted samples; α - particle energies have been converted to a depth scale in both, gallium and arsenic.

After annealing for one hour at T_a = 500 °C the measured mean range of the aluminium atoms in gallium arsenide remained unchanged at $R_p = 147 \pm 16$ *nm*. The second range moment stayed at $\Delta R_p = 65 \pm 5$ *nm*, which is the same as before annealing. No aluminium diffusion to the surface was observed, contrary to the investigated elemental semiconductors in this study. Obviously the aluminium atoms are still inside the remaining highly disordered gallium arsenide lattice after annealing where they could be incorporated on gallium sites during the regrowth which is possible, considering that AlAs and GaAs are completely miscible into each other [104].

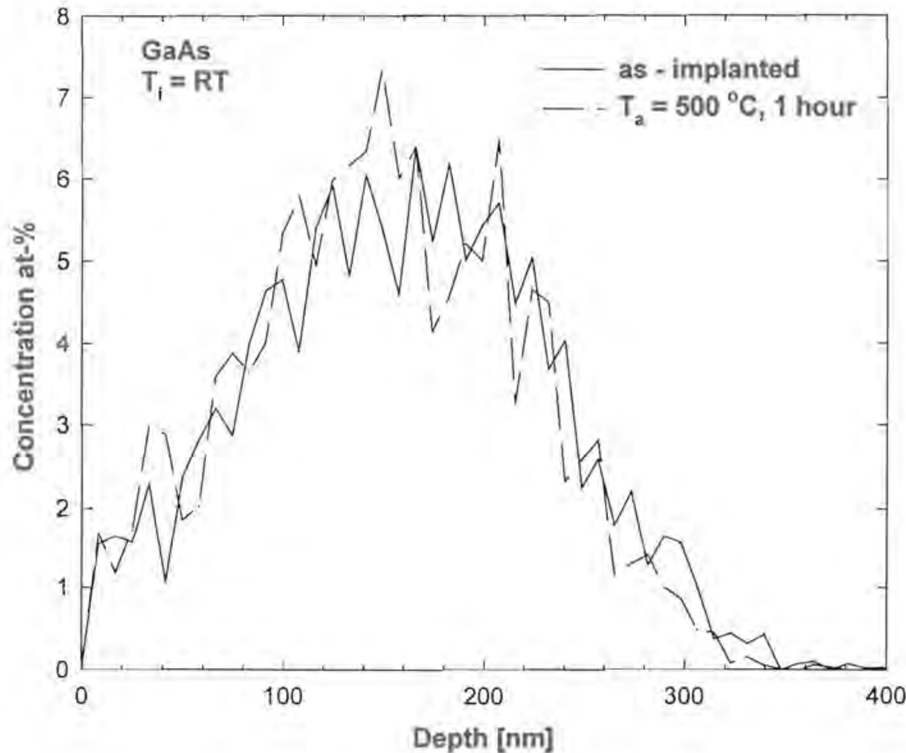

Fig. 37: Depth profiles of aluminium implanted at room temperature into gallium arsenide before and after annealing for one hour T_a = 500 °C.

An upper limit for the diffusion coefficient of $D \leq 10^{-15}$ cm^2 s^{-1} for 500 °C was extracted. However, a defect induced diffusion enhancement cannot be excluded because even an increase of the coefficient by several orders of magnitude would still be below our detection limit.

7.3.3. HOT IMPLANTATION

The channeling spectra for gallium arsenide after implantation of 5 x 10^{16} aluminium ions cm^{-2} at T_i = 250 °C are displayed in Fig. 38. The surface region was observed to be nearly defect-free. No highly disordered region, as was observed after room temperature implantation, was formed. From the shape of the channeling spectra and the low minimum yield it was concluded that radiation induced annealing plays an important role during implantation at T_i = 250 °C. This agrees well with reports on ion implantations at elevated temperatures into *III-V* compounds [91], where already during implantations at about 200 °C the point defect concentration will never exceed the critical limit for amorphisation, except probably near the end of the ion tracks, especially for light and medium mass ions (< 30

amu). Amorphous zones that are created along an ion track will shrink faster than new zones are created.

The observed minimum yield in the region beyond the surface of the as-implanted gallium arsenide sample is at χ_{min} = 10%. During annealing for one hour at T_a = 500 °C the minimum yield reduced to χ_{min} = 8% which indicates a slight recovery of the gallium arsenide lattice in the surface region, which is almost as low as the minimum yield of unimplanted gallium arsenide samples at χ_{min} = 5%. However, beyond a depth of 50 nm a rather large slope in the dechanneling yield is observed.

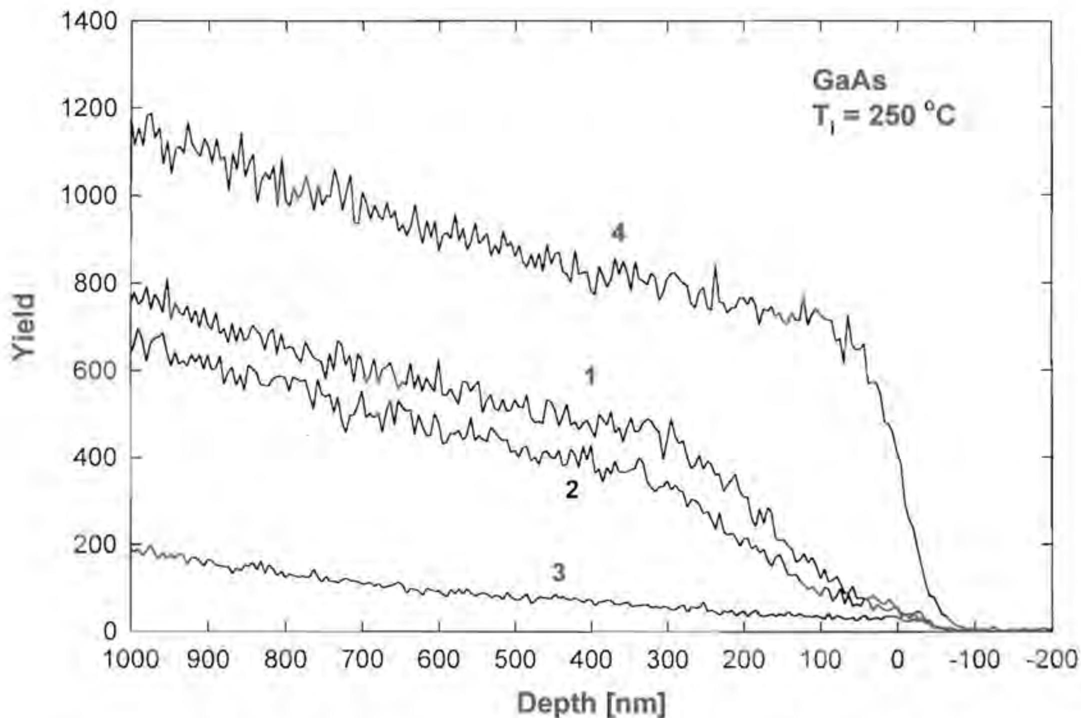

Fig. 38: Aligned backscattering spectra of gallium arsenide implantation of 5 x 10^{16} Al^+ *cm^{-2}* at T_i = 250 °C before (1) and after annealing for one hour at 500 °C (2). Also given are aligned (3) and random spectra of unimplanted samples; α - particle energies have been converted to a depth scale.

The increased slope of the dechanneling yield reaches to a depth of about 320 *nm* into the crystal, which is deeper than the detected mean range of the implanted aluminium ions. The shape of the dechanneling slope indicates extended defects such as dislocations that are

introduced during the hot implantation. The density of the dislocation network reduced slightly during annealing for one hour at 500 °C.

A similar result was already reported for implantation of 10^{15} Se^{+} cm^{-2} into gallium arsenide at T_i = 200 °C, where a discrete band of small dislocation loops and clusters was detected below the surface [92]. Their results were obtained with XTEM, RBS/channeling, SIMS and electrical measurements. They did not measure the selenium mean range in their study. However, from TRIM simulations a mean range of R_p = 174 *nm* was calculated, which is slightly deeper than our aluminium implant. The mean depth of their observed band of defects is at approximately 300 *nm* and therefore similar to the damage depth observed in this study. They concluded that the introduced defects from their hot selenium implantation were mainly dislocation loops and clusters.

The nuclear energy loss depth distribution as calculated with TRIM is displayed in Fig. 39. The nuclear energy loss is calculated by adding the ion energy losses due to recoils and the creation of phonons. As it is closely related to the introduced defects the damage range is calculated to be 165 *nm*, which is about half of the depth of our experimentally observed damage after the hot implantation. The damage depth after the room temperature implantation could not be measured because a channeling effect was not observed. However, a channeling effect was observed after annealing at 500 °C indicating crystalline regrowth from the bulk. A damage range similar to the mean range of the implanted aluminium was measured. In comparison hardly any regrowth occurred after annealing the hot implanted samples at this temperature. The damage depth remained much deeper than calculated and the slope reduced only slightly. It must be concluded that different types of defects are created during the different implantation temperatures. Radiation-induced defects in the surface region anneal out already during implantation. When considering that the hot implantation was performed at a higher dose rate than the room temperature implantation, the observed dislocation network is most probably because of denser collision cascades. Such dense collision cascades lead to shock-waves, which reach much deeper into the crystal than the mean range of the implanted ion.

Such enhanced damage ranges were previously only reported in metals [93], where they were explained with the formation of dislocations reaching much deeper than the mean range of the implanted ions due to dense collision cascades.

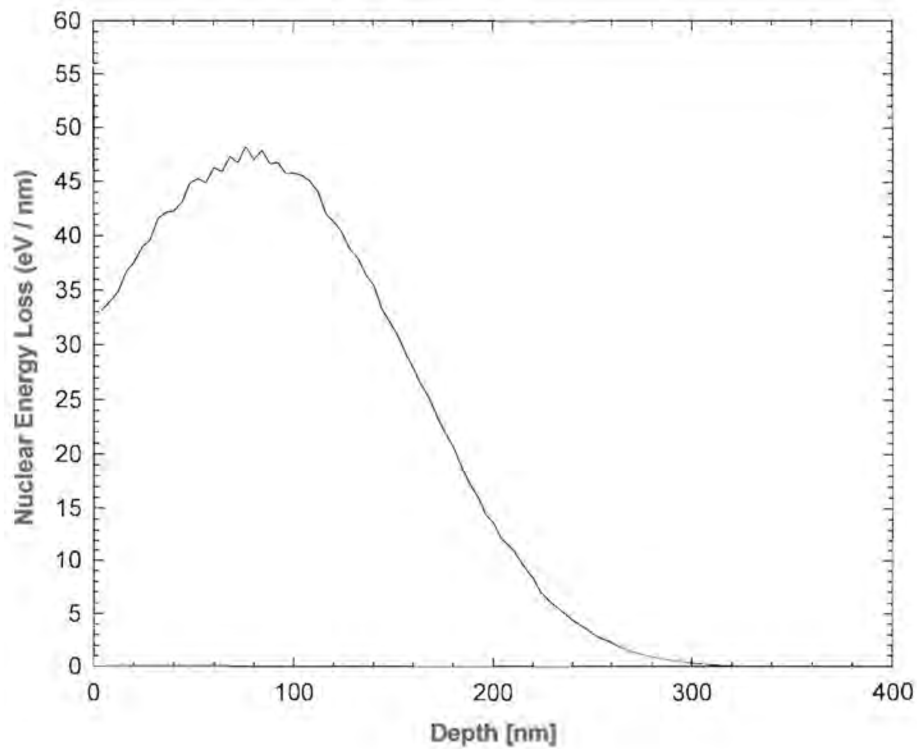

Fig. 39: Nuclear energy loss depth distribution of an aluminium ion at an energy of 120 keV in gallium arsenide as calculated with TRIM.

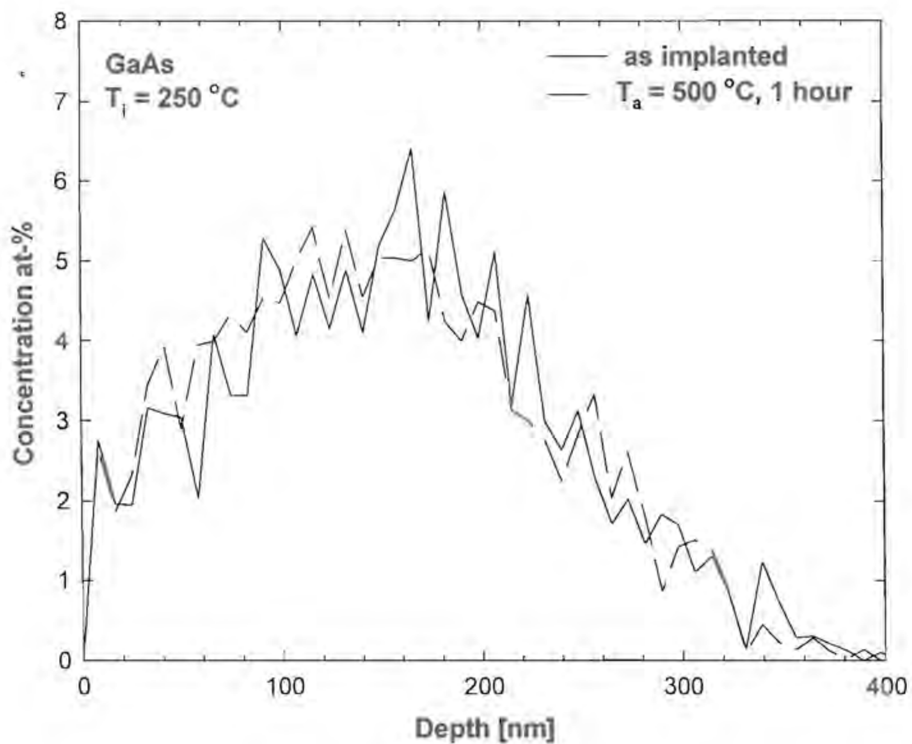

Fig. 40: Depth profiles of aluminium implanted at T_i= 250 °C into gallium arsenide before and after annealing for one hour T_a = 500 °C.

Aluminium depth profiles before and after annealing for one hour at T_a = 500 °C are displayed in Fig. 40. After implantation the mean range of the aluminium atoms is at a depth of R_p = 144 ± 16 *nm* with a second range moment of ΔR_p= 70 ± 5 *nm*. This is well within the experimental error of the values obtained for the room temperature implantation. The upper limit for the radiation-enhanced diffusion for these experimental parameters is at $D \leq 10^{-15}$ $cm^2\ s^{-1}$ by taking into account the implantation time.

After annealing for one hour at T_a = 500 °C the mean range of the implanted aluminium atoms was at R_p = 141 ± 16 *nm* with a second range moment of ΔR_p= 72 ± 5 *nm*. No visible diffusion to the surface occurred. An upper limit of the diffusion coefficient of $D \leq 10^{-15}$ $cm^2\ s^{-1}$ was extracted for annealing at T_a = 500 °C. However, the expected diffusion coefficient is not measurable with our method and therefore the obtained result is not in disagreement with previously published results.

Sample **Gallium arsenide**	**Range** R_p **[*nm*]**	**Straggling** ΔR_p **[*nm*]**	**Thermal diffusion coefficient** D **[**$cm^2\ s^{-1}$**]**
$T_i = RT$, as-implanted	152 ± 16	66 ± 5	-
$T_i = RT$, T_a = 500 °C	147 ± 16	65 ± 5	$\leq 10^{-15}$
T_i = 250 °C, as implanted	144 ± 16	70 ± 5	-
T_i = 250 °C, T_a = 500 °C	147 ± 16	72 ± 5	$\leq 10^{-15}$

Table 6: Summary of the experimental range parameters and thermal diffusion coefficients of implanted aluminium into gallium arsenide.

7.4. INDIUM PHOSPHIDE

Indium phosphide is one of the most important compound semiconductors. Many investigations were done because of its optoelectronic and high-speed digital applications. Picosecond optoelectronic switches with response times $\tau < 100$ picoseconds can be realised in indium phosphide after proton bombardment [94].

Diffusion coefficients of aluminium in indium phosphide were not found in the literature. It is important to understand the behaviour of doped semiconductors when they are exposed to heat. This study was therefore necessary to obtain information on diffusion coefficients of aluminium in indium phosphide. Decomposition occurs at annealing temperatures, typically in excess of $T_a = 600$ °C, necessary to activate implanted ions [95]. A phosphorous loss from the surface changes the stoichiometry in this compound. After phosphorous loss two phases exist in equilibrium already at room temperature. At lower annealing temperatures, e.g. for $T_a > 400$ °C, even in a nitrogen ambient a strong tendency for the surface to oxidise was observed [96,97]. To avoid these degrading effects the annealing temperatures for this study were kept at $T_a \leq 400$ °C during annealing in vacuum.

In order to investigate the in-diffusion a thin aluminium film was deposited onto a piece of indium phosphide. The obtained results are compared with those obtained after implantations at room temperature and at $T_i = 250$ °C in order to evaluate the influence of defect assisted diffusion effects in indium phosphide.

7.4.1. AL DIFFUSION INTO INDIUM PHOSPHIDE

The in-diffusion of aluminium into indium phosphide up to an annealing temperature of $T_a =$ 400 °C was investigated. An indium phosphide wafer was cut in four pieces and cleaned. Onto one of the quarters a 12 ± 4 *nm* film of aluminium was deposited. The samples of 5 x 5 mm cut from this piece were analysed before and after annealing. The depth profiles of the aluminium layer before and after annealing for one hour at $T_a = 400$ °C are shown in Fig. 41.

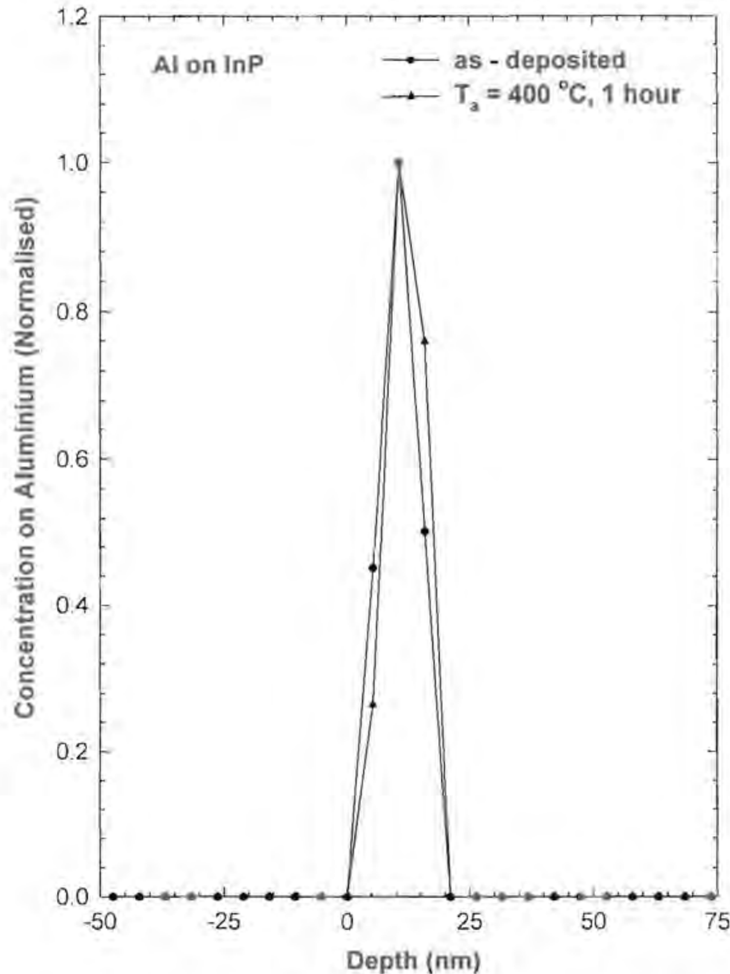

Fig. 41: Depth profiles of a vapour deposited aluminium layer on indium phosphide before and after annealing for one hour at T_a = 400 °C.

As it was the case for most of the semiconductors investigated and summarised in this chapter a slight difference in the film thickness due to inhomogenities during the vapour deposition onto the specimen is observed. However, diffusion effects are only related to the sharpness of the interface between the aluminium film and the indium phosphide wafer. The width of this interface remains within the detection limit of our method at 2.5 *nm* before and after annealing at a temperature of T_a = 400 °C. The interface remains therefore sharply defined and no change in shape of the depth profiles is observed before and after annealing. As no aluminium diffusion into the indium phosphide sample occurred within our detection limit at 400 °C, an upper limit for the aluminium diffusion coefficient in indium phosphide at $D \leq 10^{-16}$ $cm^2\ s^{-1}$ was extracted. The actual coefficient could be higher due to a possible formation of a polycrystalline In_2O_3 layer at the interface [98]. However, a surface discolouring, which is supposed to indicate the surface oxidation was not observed before and after annealing. Therefore we expect this limit for the coefficient at 400 °C to be in the right range.

7.4.2. ROOM TEMPERATURE IMPLANTATION

The implantation of 5 x 10^{16} aluminium ions cm^{-2} implanted into indium phosphide at room temperature created a highly disordered region with a thickness of X_a = 465 ± 24 *nm* at the surface of the sample as deduced from the channeling spectra in Fig. 42. The thickness of this disordered layer is about four times deeper than the mean range of the implanted aluminium atoms at R_p = 117 ± 10 *nm* (Fig. 44). The α-particle energies in the backscattering spectrum were converted to a depth scale.

After annealing for one hour at T_a = 300 °C the thickness of the amorphous layer reduced to X_a = 409 ± 22 *nm*. No further crystalline regrowth of the highly disordered layer was observed after annealing a sample for one hour at T_a = 400 °C.

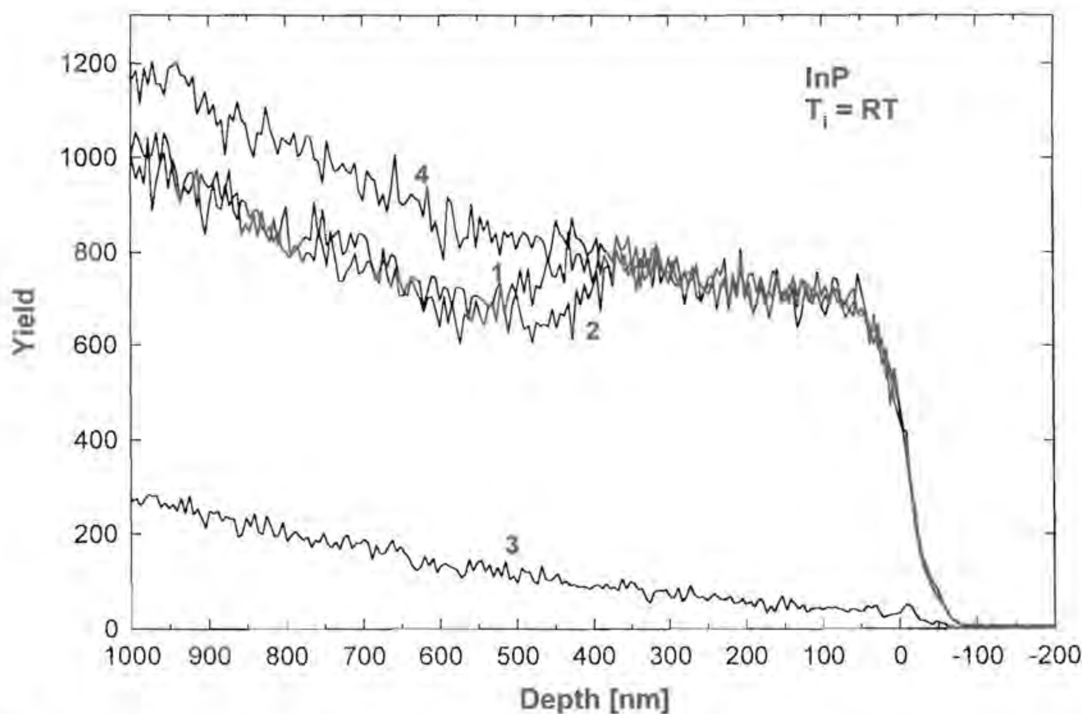

Fig. 42: Aligned backscattering spectra of indium phosphide for room temperature implantation of 5 x 10^{16} Al^{+} cm^{-2} before (1) and after annealing for one hour at 300 °C (400 °C) (2). Also given are aligned (3) and random (4) spectra of unimplanted samples; α - particle energies have been converted to a depth scale.

The nuclear energy loss depth distribution of aluminium in indium phosphide as calculated with TRIM is displayed in Fig. 43. A damage range of 192 *nm* can be extracted from this distribution. When we compare the thickness of our amorphous layer after implantation with the predicted damage range, then the observed amorphous layer is larger by more than a factor of two. In this study larger defect layers than predicted were already observed after hot aluminium implantations into gallium arsenide. After room temperature implantations of aluminium in silicon larger defect layers were also observed. It could have been also present in gallium arsenide but the samples could not be channeled.

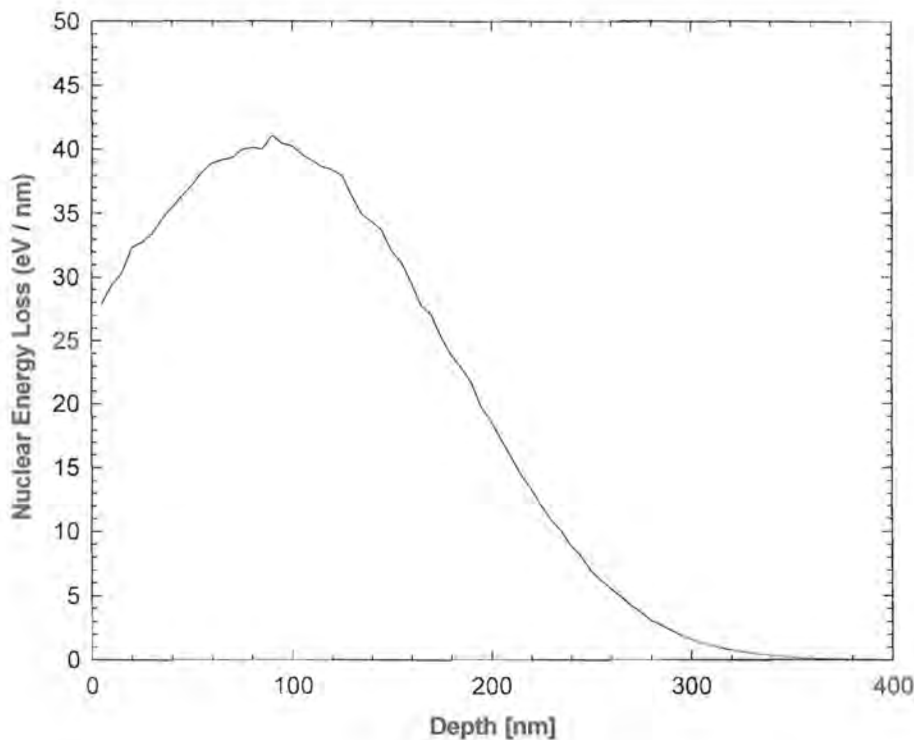

Fig. 43: Nuclear energy loss depth distribution of an aluminium ion at an energy of 120 keV in indium phosphide as calculated by TRIM.

The depth profiles of 5×10^{16} aluminium ions cm^{-2} implanted into indium phosphide at room temperature before and after annealing for one hour at $T_a = 300$ and 400 °C are shown in Fig. 44. The experimentally obtained mean range of the implanted aluminium ions before annealing was at $R_p = 117 \pm 10$ *nm* and the second range moment was at $\Delta R_p = 56 \pm 4$ *nm*.

During annealing for one hour at T_a = 300 °C the mean range of the aluminium atoms in the indium phosphide remained the same within experimental error at R_p= 113 ± 10 *nm*. The second range moment ΔR_p= 55 ± 4 *nm* also did not change within experimental error.

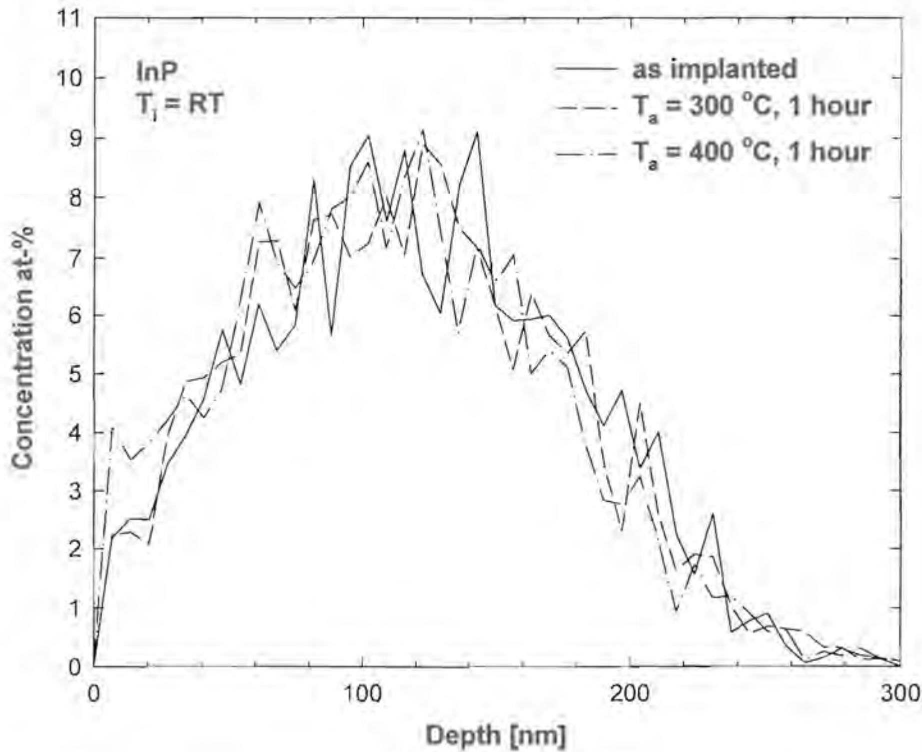

Fig. 44: Depth profiles of aluminium implanted at room temperature into indium phosphide before and after annealing for one hour at different annealing temperatures T_a.

The same results within experimental error were obtained during annealing for one hour at T_a = 400 °C. Here the mean range of the aluminium atoms was at R_p= 108 ± 10 *nm* and the second range moment at ΔR_p= 55 ± 4 *nm*. No aluminium diffusion to the surface was observed. An upper limit of the diffusion coefficient of $D \leq 10^{-15}$ cm^2 s^{-1} for T_a = 400 °C agrees well with the results obtained for in-diffusion. Diffusion coefficients at 400 °C are suspected to be much lower than the obtained upper limit because no radiation damage enhanced diffusion, which is often a few magnitudes higher than the diffusion in defect free crystals, was observed.

7.4.3. HOT IMPLANTATION

The channeling spectra for indium phosphide after implantation of 5×10^{16} Al^{+} cm^{-2} at T_i = 250 °C are displayed in Fig. 45. A complete amorphisation in the surface region, as it was observed after the room temperature implantation, did not occur during implantation at T_i = 250 °C. Radiation-induced disorder in the surface region annealed out already during implantation. When comparing the dechanneling yield beyond the surface with the results from the hot aluminium implantation into gallium arsenide in Fig. 38, it is obvious that the slope in indium phosphide is constant from the surface. A fully recovered surface layer was not observed. Apparently a constant defect density is present that reaches from the surface to a depth of about 340 *nm*. This depth is about 1.5 times deeper than the predicted defect range (see Fig. 43). From the shape of the slope of the dechanneling yield, as well as from the fact that no regrowth occurs during annealing at 400 °C, it is obvious that a dense and stable dislocation network is present to a depth of approximately 340 *nm* below the surface.

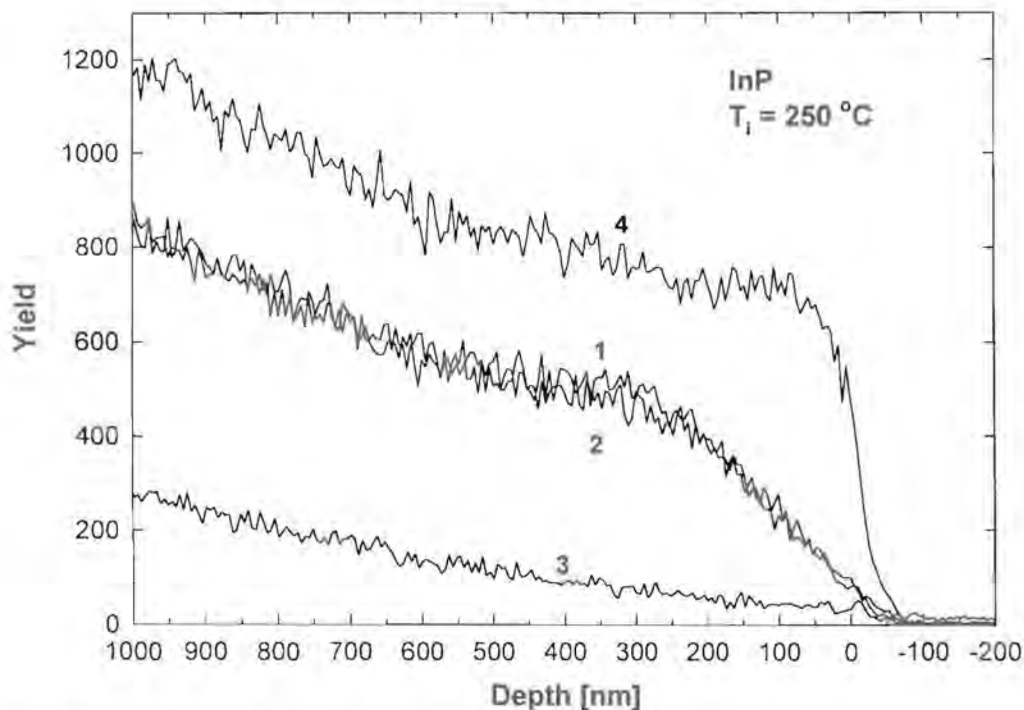

Fig. 45: Aligned backscattering spectra of indium phosphide implantation of 5×10^{16} Al^{+} cm^{-2} at T_i = 250 °C before (1) and after annealing for one hour at 400 °C (2). Also given are aligned (3) and random spectra of unimplanted samples; α - particle energies have been converted to a depth scale.

Aluminium depth profiles before and after annealing for one hour at T_a = 300 and 400 °C are displayed in Fig. 46. The mean range of the as-implanted aluminium atoms is at a depth of R_p = 109 ± 10 *nm* with a second range moment of ΔR_p= 58 ± 4 *nm*. This is well within experimental error of the range moments obtained for the room temperature implantation. As no noticeable change occurs in the range moments of the room temperature implantation and the hot implantation, the upper limit of the radiation enhanced diffusion coefficients for our experimental parameters can be extracted to $D \leq 10^{-15}$ cm^2 s^{-1}.

After annealing for one hour at T_a = 300 °C the mean range of the implanted aluminium atoms was unchanged at R_p = 109 ± 10 *nm* with a second range moment of ΔR_p= 56 ± 4 *nm*. The range moments of the implanted aluminium atoms extracted after annealing for one hour at T_a = 400 °C were at R_p = 114 ± 10 *nm* with a second range moment of ΔR_p= 55 ± 4 *nm*. No visible diffusion to the surface occurred. An upper limit for the diffusion coefficient $D \leq 10^{-15}$ cm^2 s^{-1} was obtained for 400 °C.

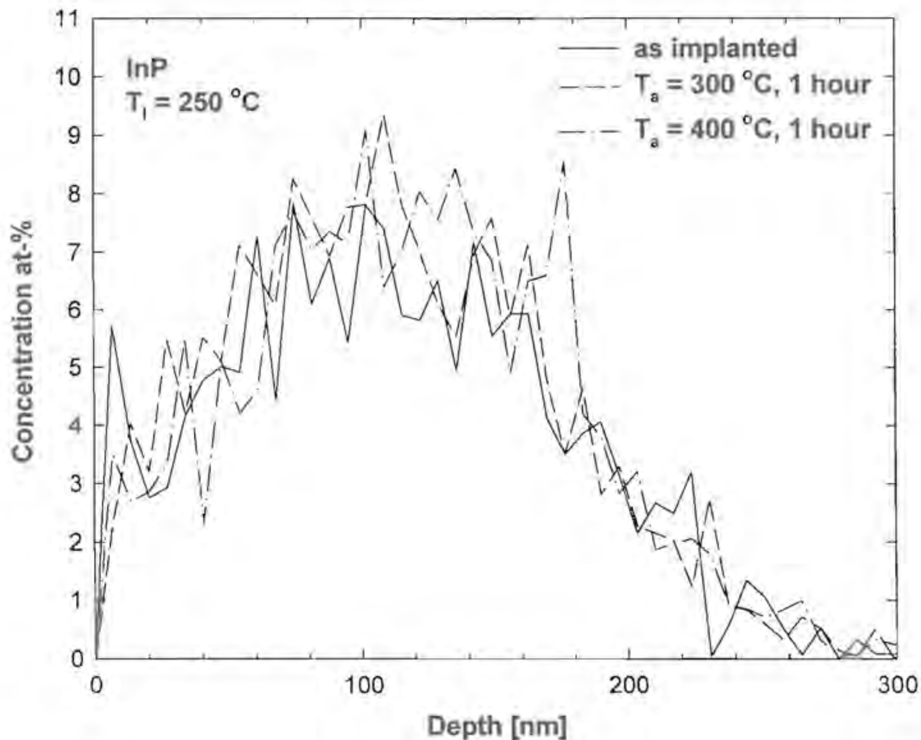

Fig. 46: Depth profiles of aluminium implanted at T_i = 250 °C with a fluence of 5 x 10^{16} cm^{-2} into indium phosphide before and after annealing for one hour at different temperatures T_a.

Sample **Indium phosphide**	**Range** R_p **[*nm*]**	**Straggling** ΔR_p **[*nm*]**	**Thermal diffusion** **coefficient** D **[$cm^2\ s^{-1}$]**
$T_i = RT$, as-implanted	117 ± 10	56 ± 4	-
$T_i = RT$, $T_a = 300$ °C	113 ± 10	55 ± 4	$\leq 10^{-15}$
$T_i = RT$, $T_a = 400$ °C	108 ± 10	55 ± 4	$\leq 10^{-15}$
$T_i = 250$ °C, as implanted	109 ± 10	58 ± 4	-
$T_i = 250$ °C, $T_a = 300$ °C	109 ± 10	56 ± 4	$\leq 10^{-15}$
$T_i = 250$ °C, $T_a = 400$ °C	114 ± 10	55 ± 4	$\leq 10^{-15}$

Table 7: Summary of the experimental range parameters and thermal diffusion coefficients of 5×10^{16} aluminium ions cm^{-2} implanted into indium phosphide.

7.5. INDIUM ANTIMONIDE

The last compound semiconductor investigated for this study was indium antimonide. This material is used for infrared detectors in the 3-5 μm wavelength range. Several studies on implantations of several elements and the resulting radiation induced damage were published previously (see chapter 6.2.3.). However, results on aluminium diffusion in indium antimonide were not found in the literature. It is important to know the behaviour of an impurity in a semiconductor under different conditions for stability predictions.

Indium antimonide is a *III-V* compound semiconductor with a melting point of T_m = 525 °C. However, at this temperature the antimony evaporates, leaving only liquid indium [99]. The eutectic temperature of this binary system is at T_e = 494 °C [100], but already at lower temperatures ($T_a \approx$ 400 °C) a surface oxidation should be prevented by annealing the compound in a nitrogen or argon ambient [101]. Due to the unavailability of a facility for anneals under protective gas flow we had to stay well below this temperature. For this investigation the in-diffusion of aluminium into indium antimonide, as well as the diffusion behaviour of implanted aluminium within this compound semiconductor was investigated at an annealing temperature of T_a = 300 °C in vacuum.

7.5.1. ALUMINIUM DIFFUSION INTO INDIUM ANTIMONIDE

The aluminium diffusion into indium antimonide was investigated at an annealing temperature of T_a = 300 °C. A 12 ± 4 *nm* aluminium film was deposited onto a quarter of a clean indium antimonide wafer. Samples cut from this piece were annealed for one hour at T_a = 300 °C. The depth profiles of the deposited aluminium film before and after annealing are shown in Fig. 47.

A slight difference in the film thickness of about $\Delta d \approx 4$ *nm* is observed. These variations in film thickness are just at the experimental detection limit of the system. The difference refers to only a few monolayers of aluminium, which is probably due to inhomogeneities during vapour depositing the aluminium film over the lateral spread of the sample.

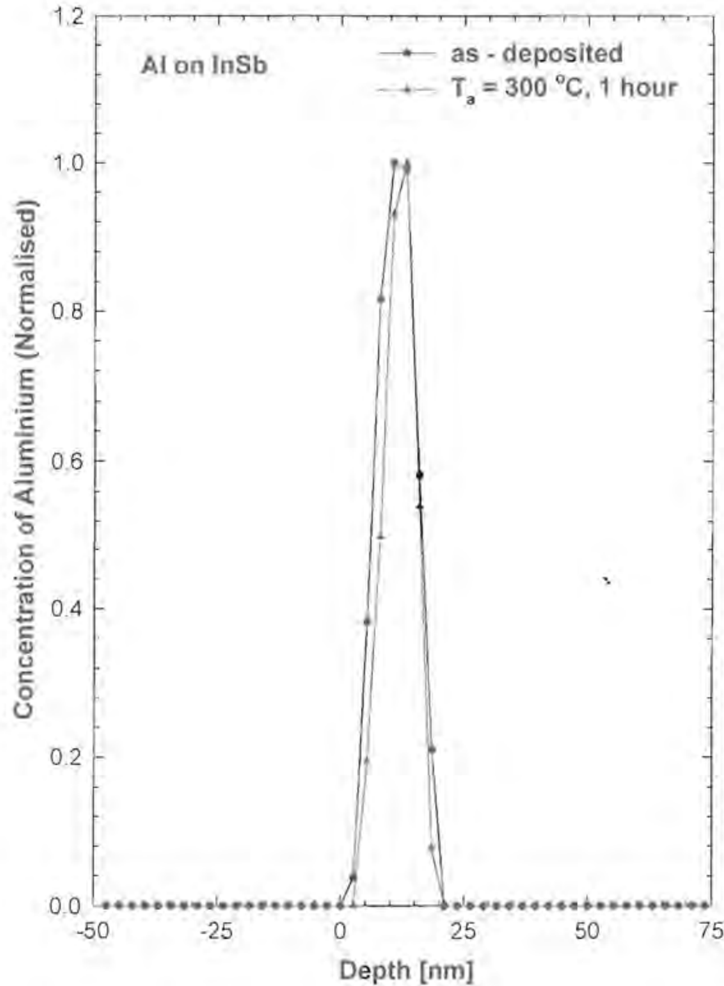

Fig. 47: Depth profiles of a vapour deposited aluminium layer on indium antimonide before and after annealing for one hour at T_a = 300 °C.

Results from the in-diffusion analysis are obtained from a possible change in width of the interface between the aluminium film and the indium antimonide substrate before and after annealing. After annealing the width remains within experimental error at 4 *nm*. Therefore the interface between the aluminium layer and the indium antimonide remains sharply defined after annealing for one hour at a temperature of T_a = 300 °C. The aluminium in-diffusion is obviously below the detection limit for our analysing method. An upper limit for the diffusion coefficient at $D \leq 10^{-16}$ cm^2 s^{-1} at 300 °C was extracted.

However, the actual aluminium diffusion coefficients at his temperature could be slightly higher than this upper limit due to native oxide layers that form at the interface before deposition of the aluminium film, and which can act as diffusion barriers [102]. In order to

bring the diffusant aluminium into direct contact with the indium antimonide, e.g. without such a diffusion barrier, it was implanted into the sample.

7.5.2. ROOM TEMPERATURE IMPLANTATION

A heavy dose ion implantation, which exceeds (3-5) x 10^{15} ions cm^{-2}, creates an irreversible structural damage in the indium antimonide crystal [86]. The observed swelling of indium antimonide after ion implantation is due to the formation of a large number of pores where the single crystal structure degraded dramatically. However, for analysis by NRA the fluence of implanted aluminium has to be high enough in order to have a moderate fluence of analysing protons combined with a high enough counting efficiency. Therefore we implanted 5 x 10^{16} aluminium ions cm^{-2} at room temperature into indium antimonide for the present study. No channeling effect was observed because of the loss of crystallinity at such a high fluence.

The depth profiles of 5 x 10^{16} aluminium ions cm^{-2} implanted into indium antimonide at room temperature before and after annealing for one hour at T_a = 300 °C are shown in Fig. 48. The experimentally obtained mean range of the implanted aluminium ions before annealing was at R_p = 115 ± 10 *nm* and the second range moment at ΔR_p= 63 ± 5 *nm*.

During annealing for one hour at T_a = 300 °C the mean range of the aluminium atoms in the indium antimonide stayed unchanged at R_p= 116 ± 10 *nm*. No change was observed in the second range moment at ΔR_p= 64 ± 5 *nm*.

Aluminium diffusion to the surface as in the case of the investigated elemental semiconductors was not observed with this compound semiconductor. Obviously the implanted aluminium atoms are still inside the highly disordered indium antimonide lattice. While in the elemental semiconductors silicon and germanium a defect enhanced diffusion was noted, such an enhancement was not observed in the investigated temperature range. One of the reasons, that there is no aluminium out-diffusion might be that SbAl and InSb are miscible in all proportions [103], to form (AlIn) Sb.

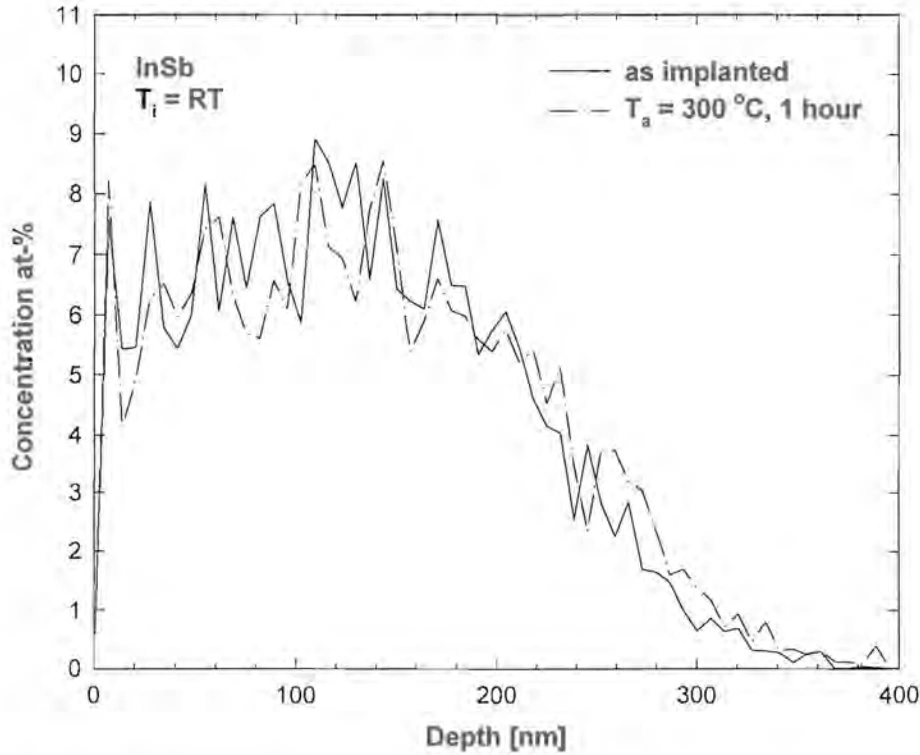

Fig. 48: Depth profiles of aluminium implanted at room temperature into indium antimonide before and after annealing for one hour at T_a = 300 °C.

Sample Indium antimonide	Range R_p [nm]	Straggling ΔR_p [nm]	Thermal diffusion coefficient D [$cm^2\ s^{-1}$]
$T_i = RT$, as-implanted	115 ± 10	63 ± 5	-
$T_i = RT$, T_a = 300 °C	116 ± 10	64 ± 5	$\leq 10^{-15}$

Table 8: Summary of the experimental range parameters and thermal diffusion coefficients of implanted aluminium into indium antimonide.

As no detectable diffusion occurred an upper limit for the diffusion coefficient at $D \leq 10^{-15}$ $cm^2\ s^{-1}$ for 300 °C was extracted. A summary of the diffusion analysis after the room-temperature implantation is listed in table 8. The obtained result is consistent with the one obtained for the aluminium in-diffusion investigation. As no diffusion was observed, we

expect the diffusion coefficient at this temperature to be much lower than the upper limit given here due to the radiation induced damage, which in the case of the elemental semiconductors enhanced the diffusion by several magnitudes.

7.5.3. HOT IMPLANTATION

After implantation of 5 x 10^{16} aluminium ions cm^{-2} at 250 °C a discolouring of the surface of the indium antimonide samples was observed. The surface appeared to be black. A surface discolouring of indium antimonide after implantation was already reported in ref. [88].

Aluminium depth profiles before and after annealing for one hour at T_a = 300 °C are displayed in Fig. 49. The shape of the implanted aluminium atoms changed dramatically during implantation at T_i = 250 °C in comparison to the room temperature implantation. The aluminium depth distribution is not gaussian anymore. The voids formed in the thermal spike of the collision cascade probably could cause the aluminium out-diffusion already during the implantation [88]. However, such a void formation would then be already expected after the room temperature implantation. We rather suspect that the outdiffusion occurs via vacancies created by an antimony loss from the surface. The loss occurs during the hot implantation and shifts this compound during annealing to a two-phase region above 157 °C, with a liquid phase containing mainly indium and the remaining solid phase [100]. After cooling the compound to room temperature an indium rich crystal remains. Considering an excess of indium with its high affinity for oxygen, the formation of In_2O_3 is expected to be responsible for the change of colour. Implanted indium antimonide surfaces are reported to oxidise easily [101]. It must be stressed, however, that a surface discolouring was not observed after the room temperature implantation.

As the aluminium depth profiles have no gaussian shape the calculation of the range moments makes no sense.

After annealing for one hour at T_a = 300 °C more aluminium diffused out of the sample as displayed in Fig. 48. This diffusion probably takes place via the above mentioned vacancies that are created by the antimony loss from the surface. Such an enhanced diffusion was not observed after the room-temperature implantation at 300 °C.

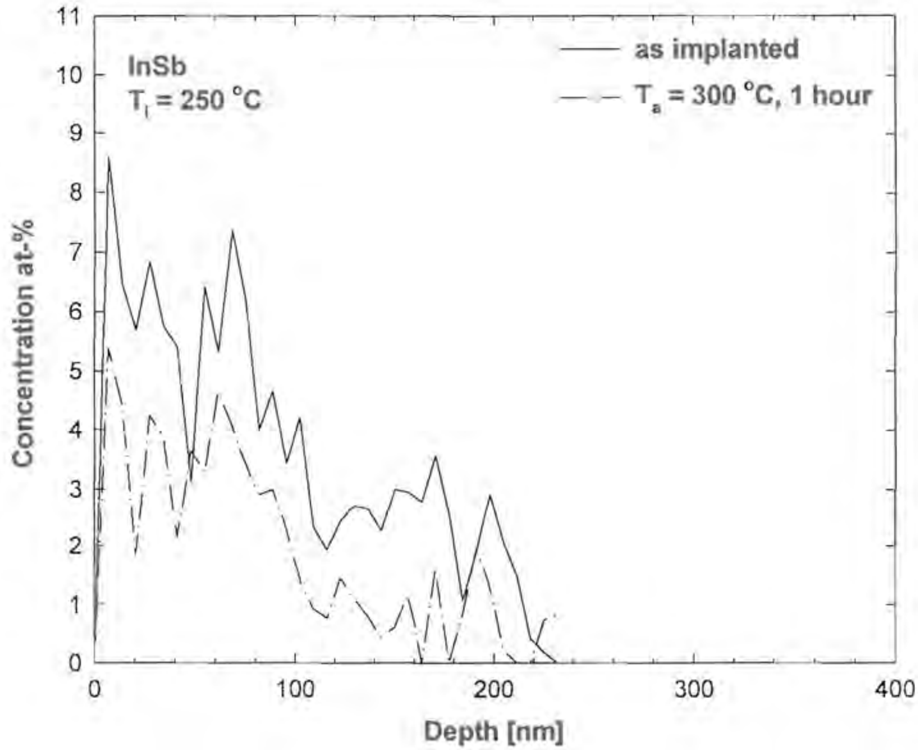

Fig. 49: Depth profiles of aluminium implanted at $T_i = 250$ °C with a fluence of 5 x 10^{16} cm^{-2} into indium antimonide before and after annealing for one hour at $T_a = 300$ °C.

A calculation of the aluminium diffusion coefficient does not make sense for the hot implantation because it will be much too large compared to the expected coefficient in an undisturbed indium antimonide crystal at 300 °C.